Open-File Report 96-4
Field Trip No. 6

# A Field Guide to the Proterozoic Anorthositic, Monzonitic, and Granitic Plutons, Laramie Range Southeastern Wyoming

By
B. Ronald Frost, Carol D. Frost, Kevin R. Chamberlain
Dept. of Geology and Geophysics, University of Wyoming
James S. Scoates
Dépt. des Sciences de la Terre et de l'Environnement, Université Libre de Bruxelles
Donald H. Lindsley
Dept of Earth and Space Science, SUNY



Colorado Geological Survey
Department of Natural Resources
Denver, Colorado
1996

# A Field Guide to the Proterozoic Anorthositic, Monzonitic, and Granitic Plutons, Laramie Range, Southeastern Wyoming

by
B. Ronald Frost, Carol D. Frost, Kevin R. Chamberlain
Dept. of Geology and Geophysics, University of Wyoming, Laramie, WY 82071
James S. Scoates
Dépt. des Sciences de la Terre et de l'Environnement - Université Libre de Bruxelles, CP 160/02 Avenue F.D. Roosevelt, 50, B-1050 Brussels - Belgium
and
Donald H. Lindsley
Dept. of Earth and Space Science, SUNY- Stony Brook, Stony Brook, N.Y. 11794

◄TOC

## INTRODUCTION

Proterozoic anorthosites and related rocks are well exposed in the high prairie and open canyons of the Laramie Mountains of southeastern Wyoming, an anticlinal foreland uplift that was formed during the late Cretaceous-Paleocene Laramide Orogeny (Figure 1). Because these rocks have been unaffected by later penetrative metamorphism and because of the accessibility of this area, the Laramie Mountains are one of the best places in the world in which to study the origin and evolution of massif anorthosites. Under the funding of the U. S. National Science Foundation, members of the faculty and students of the University of Wyoming and the State University of New York at Stony Brook have been mapping and studying the LAC since 1981 (Frost et al., 1993). This paper summarizes most of their important findings.

## REGIONAL GEOLOGY

The anorthosite bodies of the Laramie Mountains have been well known since the earliest mapping in the area (Darton et al., 1910) but only recently has it been discovered that these bodies actually represent two distinct intrusive complexes, the 1.43 Ga Laramie Anorthosite Complex (LAC) and the 1.76 Ga Horse Creek Anorthosite Complex (HCAC) (Scoates, 1994). The younger LAC, the largest of these bodies, crops out over an area of more than 800 km$^2$ (Figure 1). Primary contacts are exposed in the north and northeast, where the LAC intrudes Archean gneisses and supracrustal rocks and in the south, where the LAC has intruded Early Proterozoic metapelitic rocks, felsic gneisses and granite associated with the HCAC. The western contact of the LAC is buried under Paleozoic and Mesozoic sedimentary rocks, whereas the eastern contact has been obscured by Laramide faulting that locally has thrust the Precambrian rocks onto strata as young as Cretaceous. The difference in age between the Archean country rocks of the northern contact and the Proterozoic ones to the south reflects the fact that the LAC intruded along the Cheyenne Belt, a major crustal suture that was formed at ca. 1.76 Ga when Proterozoic island arcs and associated sedimentary sequences were sutured to the Archean Wyoming craton (Karlstrom and Houston, 1984). On the southeastern and northeastern margins, the LAC has been intruded by the Sherman batholith, a high-potassium granite that is essentially synchronous with the LAC.

The smaller and much older HCAC crops out over an area of only 140 km$^2$ between the LAC and the Sherman Batholith to the south. The gneissic granite, monzonite, and anorthosite were emplaced over a <15 m.y. interval (Scoates, 1994; Chamberlain, unpublished data). Granite and monzonite lie along the northern edge of the anorthosite and abut Early Proterozoic gneiss and the LAC The Horse Creek anorthosite (HCa) has faint-to-distinct layering that forms a broad antiform plunging to the northeast (Newhouse and Hagner, 1957)(Fig. 2). The HCa is distinct in appearance from the anorthosites of the LAC in that it has undergone a static amphibolite-grade metamorphism. Although primary igneous features are locally unaffected by this metamorphism, the pyroxenes and olivines have been altered to hornblende. On its southern and eastern margins the HCAC has been intruded by the Sherman granite, whereas its western margin is covered by Paleozoic and Mesozoic sedimentary rocks. Because of its alteration, we have not studied the HCAC to the same extent as the LAC. However, the fact that two anorthosite complexes were emplaced in the same location 300 Ma apart provides clues as to the tectonic environment of anorthosite formation

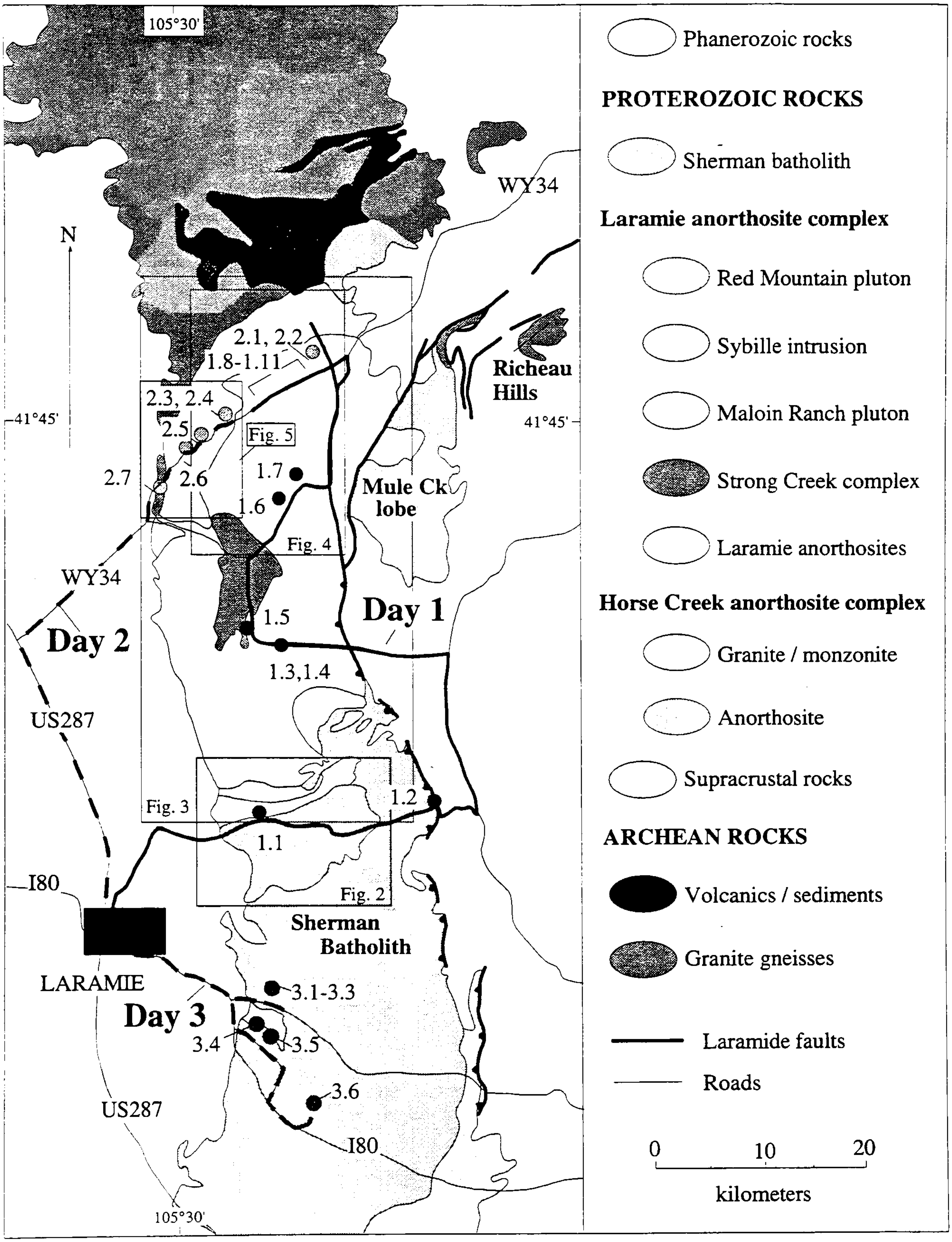


**Figure 1: Generalized Precambrian geology of the southern Laramie Range showing the extent of the Proterozoic intrusions, the stops to be made on this field trip, and the location of the detailed maps in this report.**

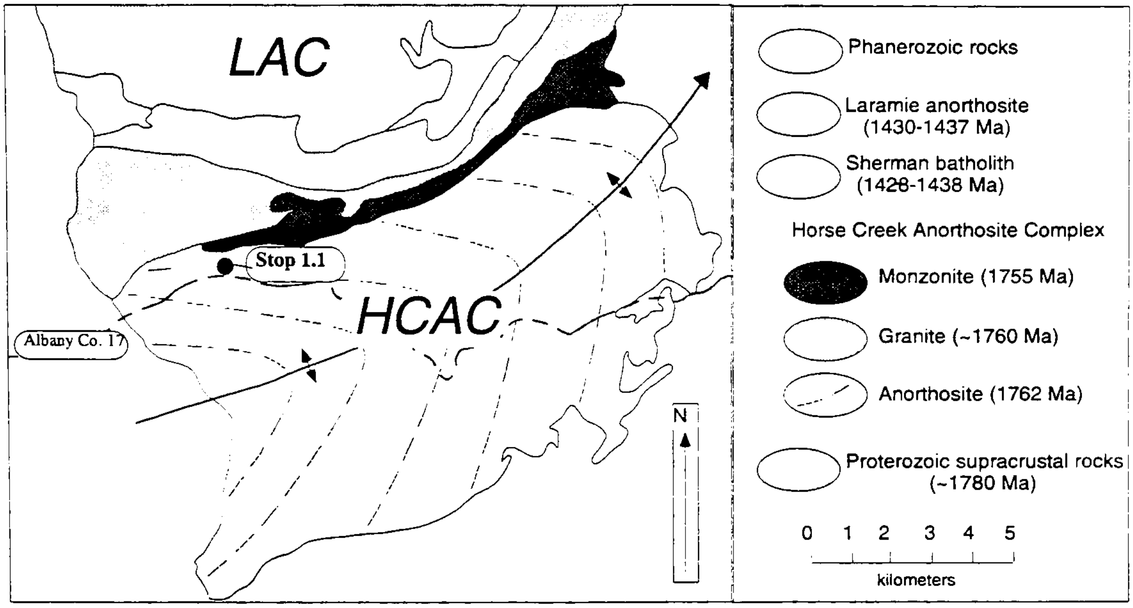


**Figure 2: Geology of the Horse Creek Anorthosite and related rocks. HCAC = Horse Creek Anorthosite Complex, LAC = Laramie Anorthosite Complex. Dashed lines show the trajectory for the layering within the Horse Creek Anorthosite. Geology after Newhouse and Hagner (1957) and Ramerathnam (1962).**

## GEOLOGIC SUBDIVISIONS OF THE LARAMIE ANORTHOSITE COMPLEX AND SHERMAN GRANITE

### Anorthosite Plutons

Based upon map patterns, plagioclase compositions, and isotopic signatures, we have distinguished three composite anorthosite plutons within the LAC (Figure 3). The oldest and most northerly pluton is the Poe Mountain anorthosite, which is a composite pluton consisting of a core of deformed, megacrystic anorthosite, surrounded by layered anorthositic cumulates (Scoates, 1994). Scoates (1994) recognized three major units of the Poe Mountain anorthosite. These included a strongly recrystallized core anorthosite, which was probably emplaced as a plagioclase-rich diapir, and a layered series consisting of a lower (inner) Anorthosite Layered Zone (ALZ) and an upper (outer) Leucogabbroic Layered Zone (LLZ) (Figure 4). Primary magmatic textures and structures, such as tabular plagioclase; ophitic pyroxenes, olivine and Fe-Ti oxides; and distinct cumulus layering are prominent in the LLZ and the upper portions of the ALZ. These features become less well defined as one moves stratigraphically downward due to the effects of high-temperature recrystallization. They are absent in the pervasively recrystallized anorthosite of the core. The layering in the layered zones dips away from the core anorthosite and becomes progressively steeper at stratigraphically higher levels. The stratigraphy of the Poe Mountain anorthosite can be followed in a broad arc overzzz a distance of more than 18 km (Figure 4). It is truncated to the south by troctolites of the Strong Creek gabbro, and in the east it disappears in an area of highly altered anorthosite adjacent to the Laramide faults along the eastern margin of the uplift.

South of the Poe Mountain anorthosite lies the Chugwater anorthosite, a megacrystic anorthosite that is distinguished from the Poe Mountain by the presence of iridescent plagioclase. Locally the Chugwater anorthosite contains meter-scaled compositional layering marked by differing abundance of ferromagnesian minerals. One horizon that is roughly a kilometer wide contains tabular plagioclase with a strong parallel alignment. However, in general the distinctive igneous textures of the Poe Mountain anorthosite, such as ophitic pyroxenes and tabular plagioclase, are absent in the Chugwater anorthosite. Instead it is dominated by megacrystic plagioclase that shows varying degrees of deformation. In places there is a fabric that is made up of oriented plagioclase laths in a matrix of neoblastic plagioclase, but it is uncertain whether this fabric is an igneous fabric or whether it is due to rotation of crystal fragments into alignment by deformation.

The southern portion of Chugwater anorthosite consists of a number of lithologically distinctive bodies that represent either nested diapirs or km-scale igneous layered zones (Figure 3). These compositional zones form a broad dome that dips steeply outward. To the north the distinction between these zones becomes less apparent as the Chugwater anorthosite becomes progressively recrystallized. The recrystallization is so intense that the contact between the core of the Poe Mountain anorthosite and the Chugwater anorthosite isvery difficult to locate; it is shown as a dashed line on Figure 3. Locally we have found that the Chugwater

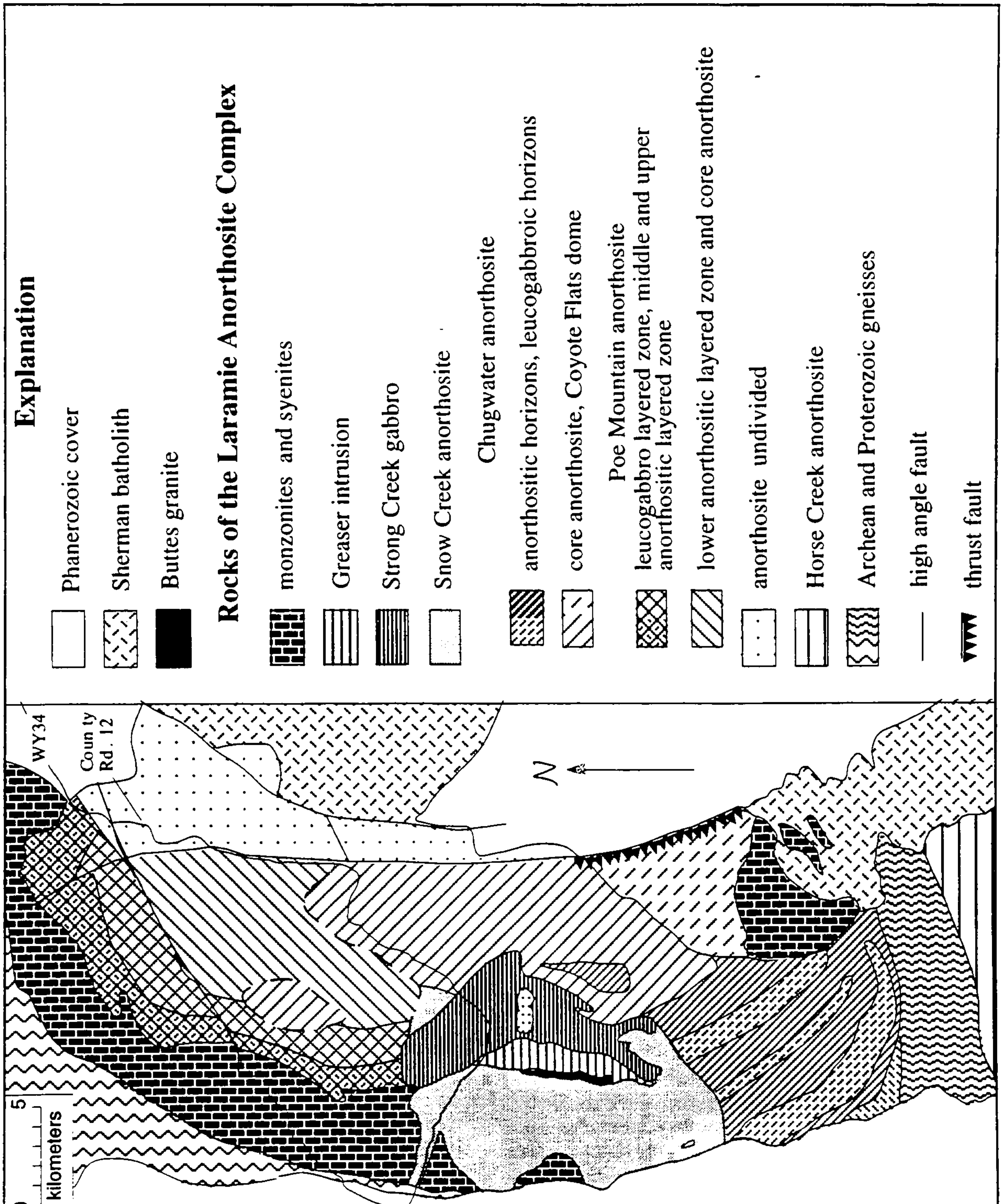


**Figure 3: Detailed geologic map of the Laramie Anorthosite Complex.**

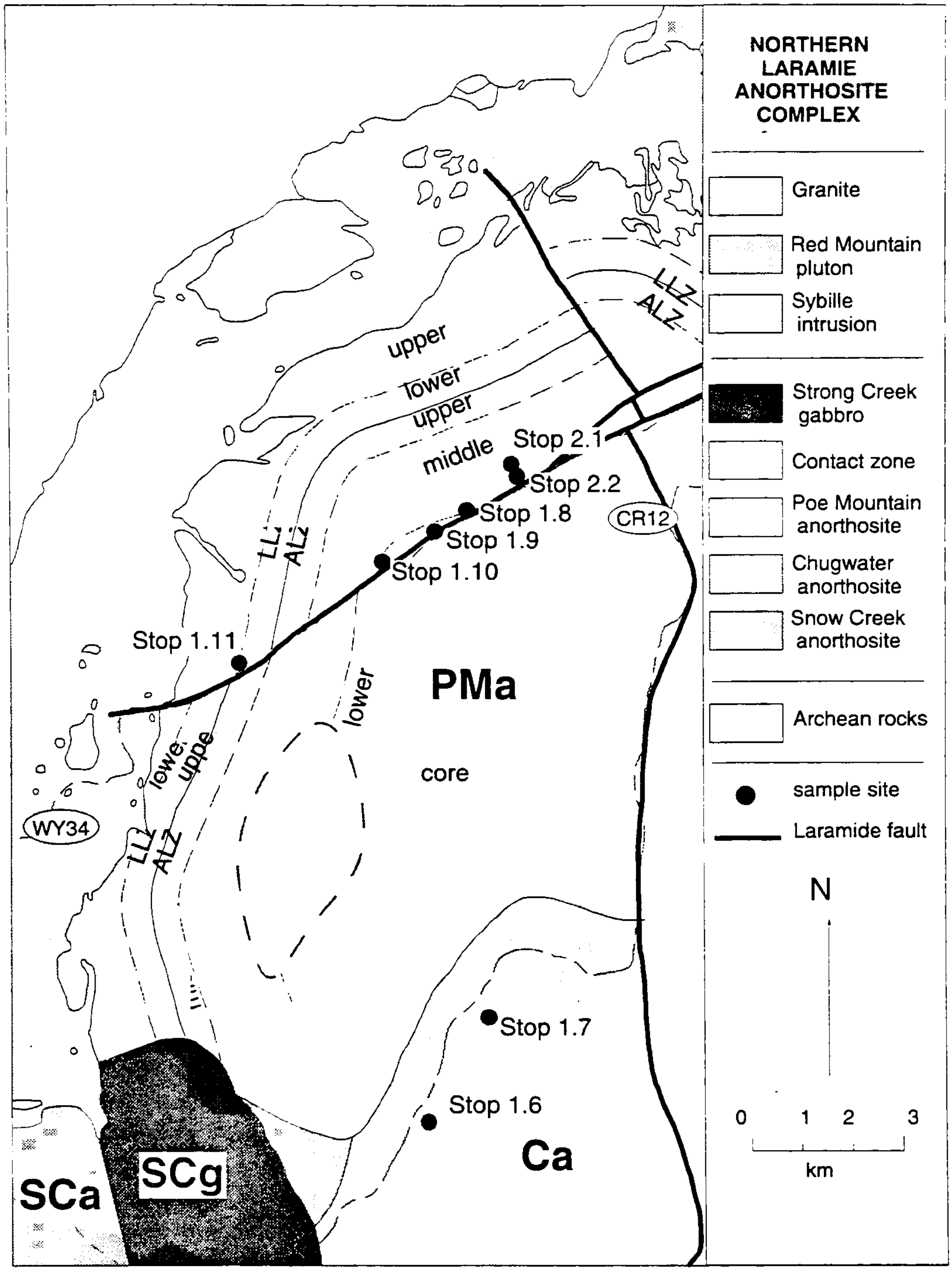


**Figure 4: Detailed geology of the Poe Mountain Anorthosite (PMa). Dashed lines show the various stratigraphic horizons in the PMa as defined by Scoates (1994). ALZ = anorthositic layered zone, LLZ = leucogabbroic layered zone. Other intrusions include Ca = Chugwater anorthosite, SCa = Snow Creek anorthosite, SCg = Strong Creek gabbro.**

anorthosite intrudes the Poe Mountain anorthosite (Figure 3). This observation not only establishes the age relations among the two plutons, but it provides us with a possible mechanism for the doming of the plagioclase-rich cumulates in the Poe Mountain anorthosite.

The western most pluton is the Snow Creek anorthosite. This poorly exposed body rarely shows a well developed fabric. The Snow Creek anorthosite, like the Chugwater anorthosite, contains iridescent plagioclase. In addition, locally it contains quartz, suggesting that it has assimilated significant amounts of crustal material. The contact between the Snow Creek anorthosite and the Chugwater anorthosite is not well defined in the field. On the map it has been placed where the good fabric of the Chugwater anorthosite disappears and is replaced by either an irregular fabric or by a fabric-free anorthosite. Based upon the fact that the mappable units of the Chugwater anorthosite are truncated by the Snow Creek anorthosite, we interpret the Snow Creek anorthosite as the youngest of the anorthosite plutons.

## Gabbroic rocks and ferrodiorite

Gabbroic rocks and ferrodiorites form dikes and small bodies throughout the anorthosite complex. Rock types range from high-Al gabbro (HAG) (Mitchell et al., 1995), through troctolite, to ferrodiorite and monzodiorite (fine monzonite of Fuhrman et al., 1988 and Kolker and Lindsley, 1989). The HAG is generally fine grained and equigranular. It consists of plagioclase($An_{50-60}$), augite, olivine ($Fa_{46-40}$) and orthopyroxene with lesser amounts of biotite, apatite and Fe-Ti oxides (Mitchell et al., 1995). HAG olivine and pyroxenes are the most magnesian in the LAC, which is a primary reason why they are considered to represent parental magma compositions to the anorthositic rocks of the LAC (Mitchell et al., 1995). HAG usually occur as small dike-like bodies that are rarely more than a meter wide and 10 meters long. Most commonly they intrude anorthositic rocks, but they also have been found intruding the country rocks in the contact aureole. In the central portion of the Sybille pluton there are a number of moderate sized inclusions (on the scale of hundreds of meters) of HAG that range in grain size from fine to coarse. We interpret these as a dismembered gabbroic intrusion with chilled margins.

Ferrodiorites form a family of rocks that range from ferrodiorite (Fdi) (with inverted pigeonite-augite-plagioclase-Fe-Ti oxides), through olivine ferrodiorite (Ofdi) (with olivine-inverted pigeonite-augite-plagioclase-Fe-Ti oxides) to olivine-oxide ferrodiorite (Oofdi) (with olivine-Fe-Ti oxides-augite-plagioclase). Mineral compositions are similar in all three rock types: plagioclase has the same composition in all rocks ($An_{38-42}$) and olivine (or fictive olivine in the Fdi) is ~$Fa_{75}$ (Mitchell et al, 1996). The ferrodiorite family of rocks are interpreted to have formed from the residual liquids of the anorthosite complex (Mitchell et al., 1996).

Locally throughout the anorthosite there are small (usually on the order of several hundred meters in the largest dimension) troctolite or olivine gabbro bodies. These are somewhat more evolved than the HAGs (for example olivine is $Fa_{50-60}$ and olivine is $An_{45}$ in troctolite from the Sybille Pit; Bolsolver, 1985). These bodies are intimately associated with massive Fe-Ti oxide deposits, rocks that consist almost entirely of titanomagnetite and ilmenite. We believe that the Fe-Ti oxides were derived from these melts, either by unmixing of an Fe-rich melt (Epler, 1987), or by mechanical settling. Most of the massive Fe-Ti oxide bodies are too small to show on the maps in this paper. Two of the most distinctive localities, the Sybille Pit (Bolsover, 1986; Epler, 1987) and Iron Mountain (Eberle, 1983) were mined in the 1960s for heavy aggregate (Frost and Simons, 1991). We consider the troctolite and olivine gabbro bodies to have formed from liquids from which some plagioclase has been extracted but which do not lie as far along the liquid-line-of-descent as the ferrodiorites.

The largest ferrodiorite and gabbro bodies occur in the center of the complex as the Greaser intrusion and the Strong Creek gabbro, respectively (Figure 5). These bodies are but weakly deformed and intrude the Poe Mountain, Chugwater, and Snow Creek anorthosites. Consequently they represent the last pulses of mafic plutonism in the LAC. The Greaser intrusion is a body measuring 8 km by 1 km that consists mostly of ferrodiorite with numerous dikes of high-Al gabbro. The Strong Creek gabbro is an undeformed coarse-grained gabbro covering an area of 10 $km^2$ that lies to the east of the Greaser intrusion. The western limits of the Strong Creek gabbro are relatively well defined, but the eastern and northern margins can only be located approximately. In these areas the intrusion is littered with inclusions of anorthosite, which become more abundant as one moves away from the core of the body. Because the anorthosite inclusions form resistant outcrops whereas the host gabbro forms grassy slopes, it is impossible to identify where the network of gabbro separating isolated blocks of anorthosite dies out. Analyses of the Strong Creek gabbro (Mitchell, 1993) show that is has a substantial range of Mg# (0.67-0.26), indicating that it may record a significant degree of differentiation.

## Monzonitic plutons

Three late monzonitic plutons lie around the margins of the anorthositic plutons. These include the Sybille pluton and the Red Mountain pluton on the north and the Maloin Ranch pluton on the southeast. Rocks in these plutons range in composition from ferrodiorite and monzodiorite (monzodiorite = fine monzonite of Fuhrman et al., 1988 and Kolker and Lindsley, 1989) to granite, although the main rock in each pluton is a monzonite or monzosyenite. The ferrodiorite and monzodiorite occur as inclusions and dikes, mainly along the margins where the plutons contact the anorthosite. Fuhrman et al. (1988) and Kolker and Lindsley (1989) mapped considerable extents of porphyritic monzonite that was texturally intermediate between the monzodiorite and the monzosyenite. Locally granite occurs along the margins where these plutons abut country rock. In the Sybille pluton zones of porphyritic granite (usually only 10 meters or so in thickness) only occur adjacent to inclusions of granitic country rock. The outer margins Red Mountain pluton has a mappable unit of porphyritic granite that appears to have formed by assimilation of country rock melt (Anderson, 1995) and the upper portions of Maloin Ranch pluton also grades into granite (Kolker and Lindsley, 1989).

Unlike the anorthositic plutons, all of which show various degrees of crystal-plastic deformation, the monzonitic plutons are undeformed. The Sybille and Maloin intrusions, however, show different levels of exposure. The present level of exposure is clearly near the top of the Sybille Pluton, for it is riddled with numerous inclusions of country rock, particularly near its northern contact (Figure 5). The presence of these inclusions indicates that stoping was an important component in its emplacement. In contrast, a tilted section through the Maloin Pluton appears to be exposed. At the base of the pluton lie remnants of ferrodiorite and high-Al gabbro that were injected along the floor of the intrusion (Kolker and Lindsley, 1989), and the intrusion grades upward into Sherman granite.

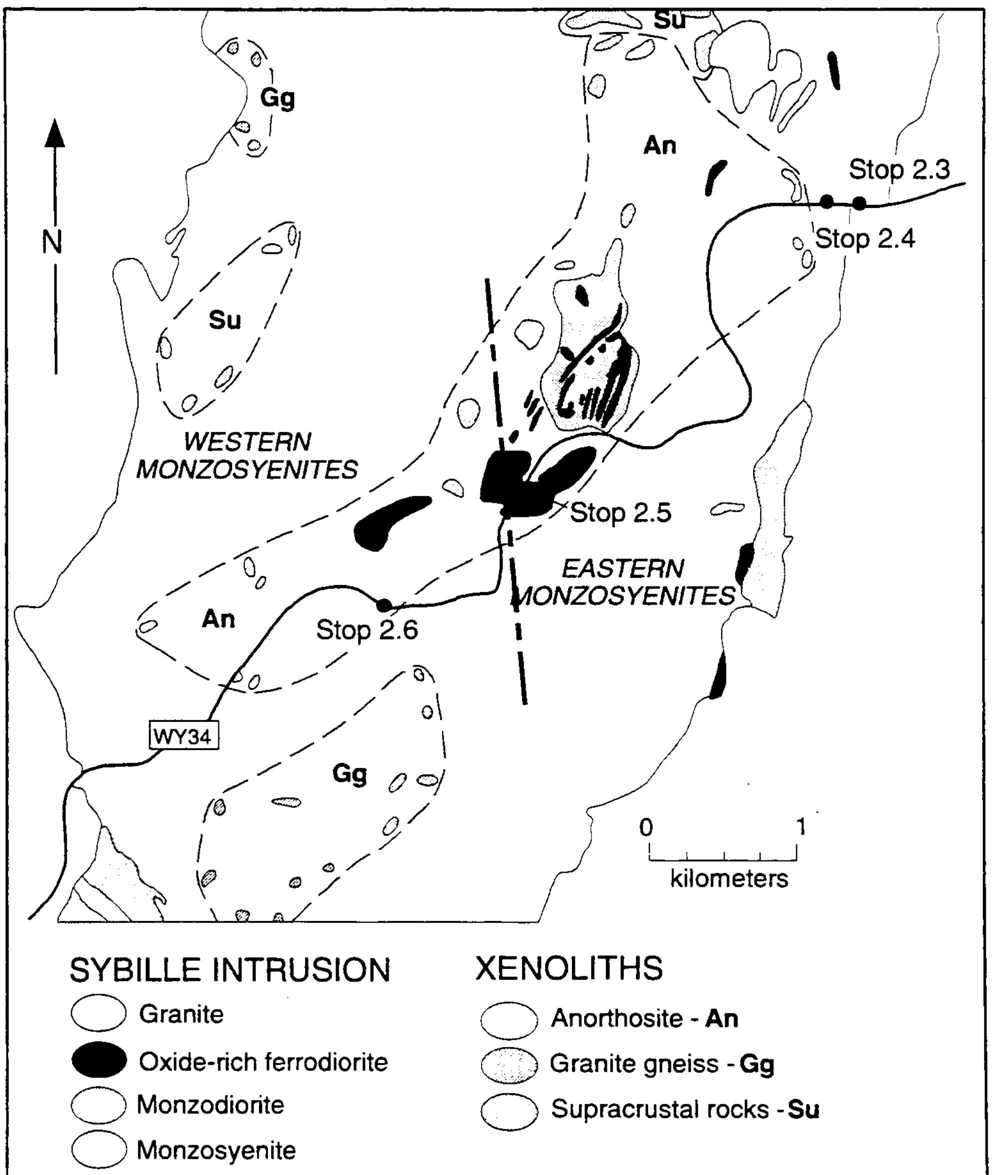


**Figure 5: Geology of the southern portion of the Sybille Pluton showing the location of stops on the field trip. Map modified from Scoates et al. (1996).**

## Sherman batholith

The Sherman batholith is spatially and temporally associated with the Laramie Anorthosite Complex. The batholith is exposed across 1300 km$^2$ of the southern Laramie Range in southeastern Wyoming and the Front Range of northern Colorado. Smaller exposures lie in the Medicine Bow Mountains and Sheep Mountain to the west. The northernmost lobe of the Sherman batholith is the Mule Creek lobe, which is exposed immediately east of the Poe Mountain anorthosite (Fig 1).

The Sherman batholith is composed of three main rock types. The first of these is the Sherman granite, a coarse-grained, biotite-hornblende granite. The reddish-orange granite weathers deeply, forming a thick grus. Microcline is megacrystic, and in places is ovoid, rimmed by plagioclase creating a rapakivi mantle. The Sherman granite grades into a porphyritic variety, known informally as the porphyritic granite. Together, the Sherman granite and the porphyritic granite are the dominant rock types in the batholith. In some areas, the porphyritic granite appears to be a hybrid rock formed by the interaction of granitic and monzodioritic or gabbroic magmas. This hybrid rock forms an extensive, mappable unit in the Virginia Dale area of northern Colorado (Eggler, 1968). The third granite unit is the Lincoln granite, a medium-grained equigranular granite that contains a very low proportion of mafic minerals (principally biotite). In many places it forms late dikes and sills, although it also may be found as inclusions in the Sherman granite. The granites are petrographically very similar to the granite found on the margins of the Red Mountain pluton and the Maloin Ranch pluton.

Monzodiorite dikes and pods constitute less than 1% of the rocks in the Sherman batholith. Contact relations with the granitic rocks are varied: in some areas they are sharply cross-cutting, in other areas the contacts are gradational with porphyritic granites, and lobate/cuspate with the Lincoln granite. The monzodiorites are similar to the ferrodiorites of the Laramie Anorthosite Complex, although most are geochemically more evolved than the LAC ferrodiorites. Furthermore, monzodiorite inclusions in the Sherman batholith contain hornblende and biotite as the main ferromagnesian silicates, whereas the similar rocks from the LAC usually have only pyroxene and olivine.

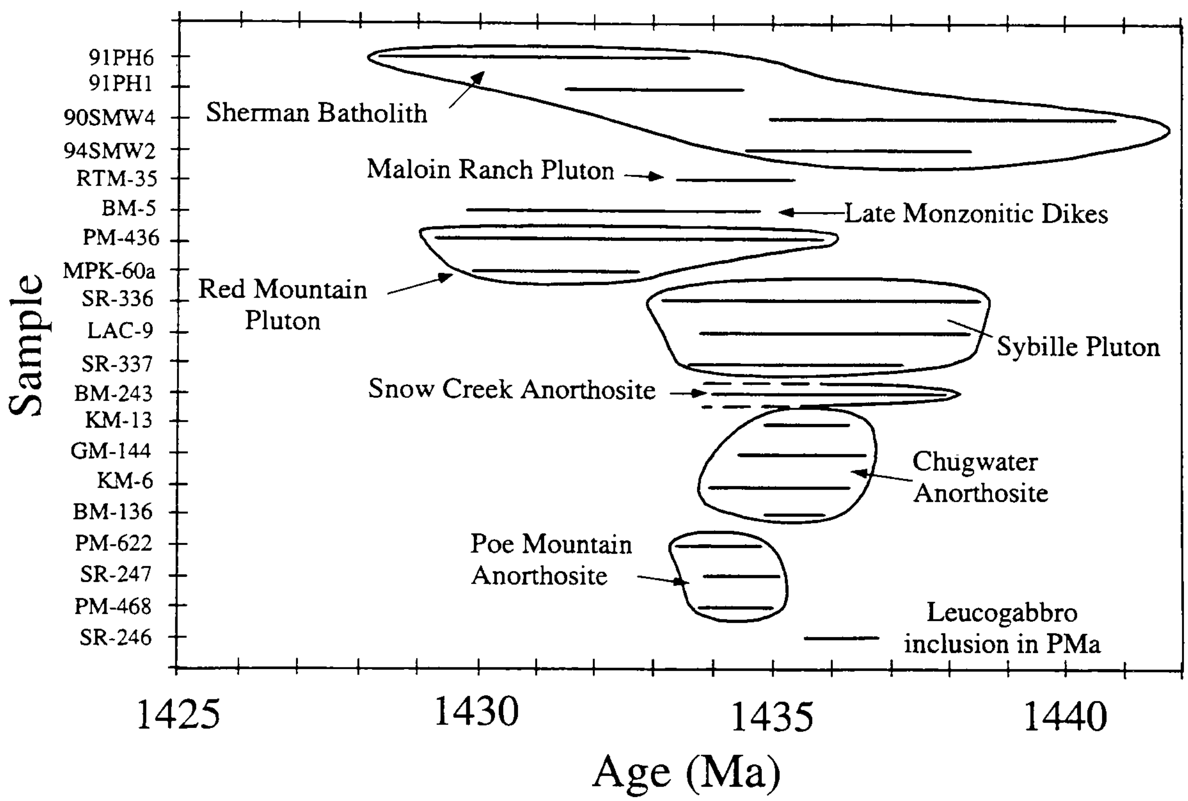


**Figure 6. Geochronology of the Laramie Anorthosite Complex and Sherman batholith. Data from Frost et al. (1990), Scoates (1994), Scoates and Chamberlain (1995), and unpublished data of Chamberlain, C.D. Frost, and Scoates.**

## GEOCHRONOLOGY OF THE LAC AND SHERMAN BATHOLITH

U-Pb ages have been obtained from zircon or baddeleyite from twenty samples of the Laramie Anorthosite and the Sherman Granite (Frost et al., 1990; Scoates and Chamberlain, 1995; Verts et al., 1996; Scoates; Chamberlain, unpublished data). They show that the LAC and Sherman batholith were intruded at around 1435 Ma (Figure 6). The Chugwater, Poe Mountain, and Snow Creek anorthosites have ages that lie within error of each other at 1436-1433 Ma. The age of Snow Creek anorthosite is a minimum because, unlike all the other samples from the LAC, U-Pb data from Snow Creek zircons provide evidence of older, inherited components. The oldest age we obtained from the anorthositic rocks came from sample SR-246, a leucogabbro xenolith within the Poe Mountain anorthosite (Scoates and Chamberlain, 1995).

Monzonitic rocks from the Sybille pluton, which clearly intrude the Poe Mountain and Snow Creek anorthosites, have ages that overlap those of the anorthosites. A comparison of the U-Pb zircon ages and their uncertainties shows that the Sybille pluton must have been emplaced within 2 m.y. of the emplacement of the Poe Mountain anorthosite. The Maloin Ranch Pluton has an age that overlaps that for Sybille (1433-1435 Ma). Since they are nowhere in contact we cannot establish relative age relations and consider them to be coeval. In contrast, field relations require that the Red Mountain pluton is younger than the Sybille, as indicated by a U-Pb zircon age from MPK-60a (1430-1433 Ma) (Frost et al., 1990; Verts et al., 1996), the main fayalite monzonite unit in the intrusion. The other dated sample interpreted to be part of the Red Mountain pluton, PM-436 is a monzodiorite from a composite dike that intrudes the Poe Mountain anorthosite. It may be as much as 0.5 m.y. younger.

The main rock types composing the Sherman batholith, the coarse-grained Sherman granite (91PH1) and medium-grained Lincoln granite (91PH6), were emplaced at approximately the same time as the Red Mountain pluton. A monzonite inclusion (90SMW4) and a gneissic granite (94SMW2) appear to be a few million years older. It thus appears that the Sherman batholith was a magmatic system that operated for a longer time than did the Laramie Anorthosite Complex. This also is suggested from field relations, for the Sherman granite is intimately intermixed with the upper portion of the Maloin Pluton, whereas it cuts the LAC in other areas.

## MINERAL CHEMISTRY AND INTENSIVE PARAMETERS OF THE LAC

The rocks of the Laramie Anorthosite Complex are markedly anhydrous. The only hydrous ferromagnesian silicates found in the complex are Ti-rich biotite, which is found locally in association with Fe-Ti oxides in the gabbros and anorthosites, and hornblende, which is found in some samples of the monzosyenites. There is a distinct iron-enrichment trend in the ferromagnesian silicates within the complex (Figure 7). The anorthosites and gabbros contain the most magnesian silicates. Pigeonite is the stable low-Ca pyroxene in about half of the samples, although some rocks have low enough Fe/(Fe+Mg) ratios to have orthopyroxene stable instead (Scoates, 1994). Ferrodiorites have pigeonite as the major low-Ca pyroxene, whereas the oxide ferrodiorites (OFdi) lack pigeonite and have olivine and augite as the major ferromagnesian silicates (Mitchell et al., 1996). The clinopyroxene in the OFdi is extensively exsolved and when reconstructed from microprobe analyses has compositions that lie atop the augite-pigeonite solvus. Such low-Ca pyroxenes are also found in the fine monzonites (Fuhrman et al., 1988). Low-Ca pyroxene is absent in the more iron-enriched monzosyenites, where fayalite and quartz are present instead (Fuhrman et al., 1988; Kolker and Lindsley, 1989; Anderson, 1995).

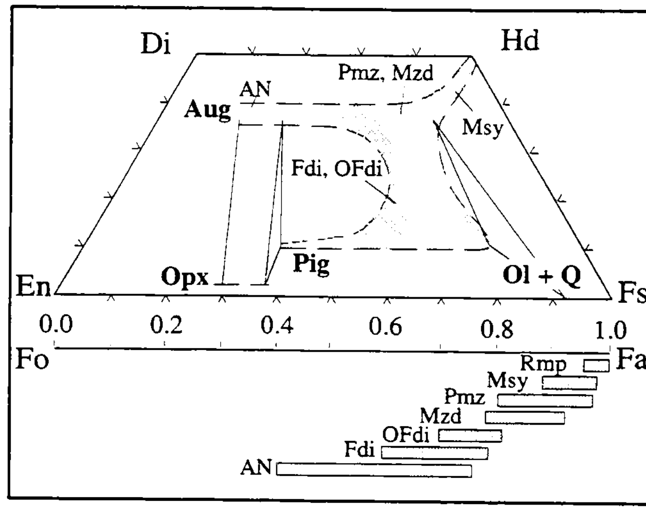


**Figure 7: Composition trends in the ferromagnesian silicates from the Laramie Anorthosite Complex. AN = anorthosite and gabbro, Fdi = ferrodiorite, OFdi = oxide ferrodiorite, Mzd = monzodiorite, Pmz = porphyritic monzonite, Msy = monzosyenite, RMP = Red Mountain pluton. Data from Fuhrman et al. (1988), Kolker and Lindsley (1989), Anderson (1995).**

The Fe/(Fe+Mg) ratio at which the transition from pigeonite to fayalite + quartz takes place is pressure-dependent and this geobarometer allows us to estimate that the northern portion of the LAC was emplaced at around 3 kilobars (Fuhrman et al., 1988). This pressure estimate is in good agreement with pressures determined from the contact aureole at Morton Pass (Grant and Frost, 1990), on the northwest margin of the complex, and at Tunnel Road, on the northeast (Spicuzza, 1990). The Maloin Ranch pluton on the southern margin of the complex appears to have been emplaced at a pressure closer to 4 kilobars (Kolker and Lindsley, 1989). The magmatic temperature cannot be determined, but, based upon the Fe/(Fe+Mg) ratio at which opx inverted to pigeonite (Lindsley and Frost, 1992), the more magnesian anorthosites and gabbros solidified at temperatures around 1100°C. The monzodiorites appear to have solidified at temperatures somewhat in excess of 1000°C, while the monzosyenite plutons crystallized at temperatures around 950° (Fuhrman et al., 1988; Kolker and Lindsley, 1989; Anderson, 1995).

The coexistence of Fe-Ti oxides with olivine and pyroxenes allows us to constrain closely the oxygen fugacity (Figure 8) Figure 8 is a polythermal plot similar to that presented by Frost and Lindsley (1992) in which temperature drops from around 1100°C at $X_{Fe}$ = 0.5 to 1000°C at $X_{Fe}$ = 1.0. This is very close to the temperatures estimated for the various portions of the intrusion where olivines of these compositions would occur. Although some rocks from the LAC lack olivine and some anorthosites, particularly the Snow Creek anorthosite, lack magnetite, the vast majority of the rocks from the LAC contain the assemblage olivine - augite - orthopyroxene (or pigeonite) - magnetite - ilmenite. This assemblage is a derivation of the Mg- and Ca- free assemblage quartz-ulvöspinel-ilmenite-fayalite (i.e. QUILF) (Frost et al., 1988) and it allows one to monitor oxygen fugacity in a rock merely by following the Fe/(Fe+Mg) ratio of the silicates (Lindsley and Frost, 1992). The common occurrence of olivine in the LAC indicates that, throughout its crystallization history, the magma forming the LAC followed close to the olivine-saturated QUILF surfaces, falling from conditions slightly above the fayalite-magnetite-quartz (FMQ) buffer to oxygen fugacities 1 to 2 log units below FMQ for the most iron-enriched rocks. This relative reduction in oxygen fugacity is a product of the iron-enrichment that accompanies the evolution of these magmas and is probably responsible for the absence of magnetite from the most evolved plutons (Fuhrman et al., 1988).

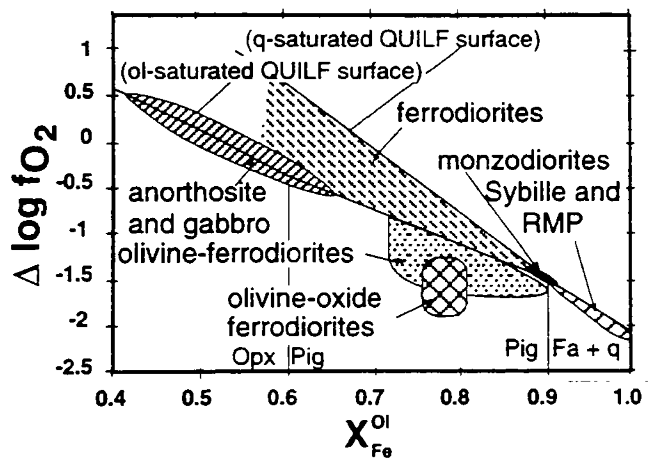


**Figure 8: Plot showing how equilibrium oxygen fugacity varied as a function of composition in rocks of the Laramie Anorthosite Complex. $X_{Fe}$ gives the composition of the olivine in the rock or the composition of the olivine that could have coexisted with the pyroxenes in the rock (see Frost and Lindsley, 1992). Plot assumes that P = 3000 bars and that the temperature falls from 1100°C at $X_{Fe}$ = 0.5 to 1000°C at $X_{Fe}$ = 1.0.**

The crystallization of the monzosyenites at such high temperatures implies that the magmas were very dry. This is seen both in the paucity of hydrous phases in these rocks and in the composition of the fluid inclusions. Frost and Touret (1989) found that the primary fluid inclusions from the Sybille monzosyenite were nearly pure $CO_2$ and that there were also abundant salt inclusions, suggesting that the fluids were so dry that chlorides came out as an immiscible melt rather than as brine. Similar $CO_2$-rich fluid inclusions were found in the Red Mountain Pluton (Anderson, 1995). The occurrence carbonaceous fluids and the reduced nature of the rocks explains the presence of graphite on grain boundaries in anorthosites and monzonites from the LAC. Frost et al. (1989) postulate that this grain-boundary graphite was produced by reduction of a $CO_2$-rich fluid by reaction with the Fe-Ti oxides during cooling.

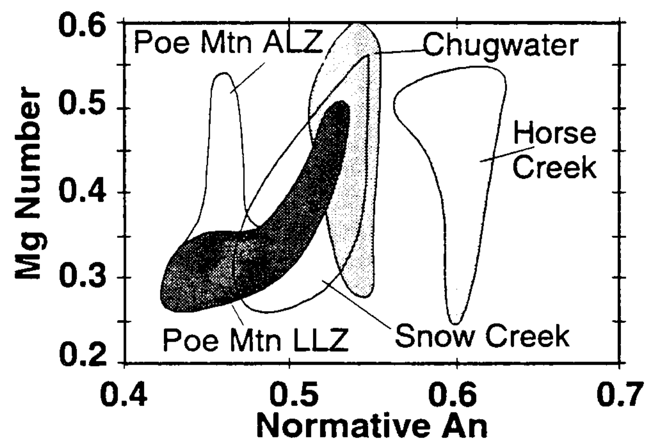


**Figure 9: Plot of Mg number versus normative An showing that most of the plutons, have distinctive compositional ranges. Data from Scoates (1994) and unpublished data from C.D. Frost.**

# GEOCHEMISTRY OF THE LARAMIE AND HORSE CREEK ANORTHOSITE COMPLEXES AND THE SHERMAN BATHOLITH

## Horse Creek and Laramie Anorthosite Complexes

### Major Elements

Like most anorthosites, the anorthositic rocks of the LAC are rich in $Al_2O_3$, CaO, and $Na_2O$, and relatively poor in Fe and Mg (Scoates, 1994). A plot of normative An vs. Mg# (Mg/(Mg+$Fe^{2+}$)) effectively discriminates the various anorthositic intrusions in the Laramie Mountains (Figure 9). Evolution of anorthosite plutons can produce

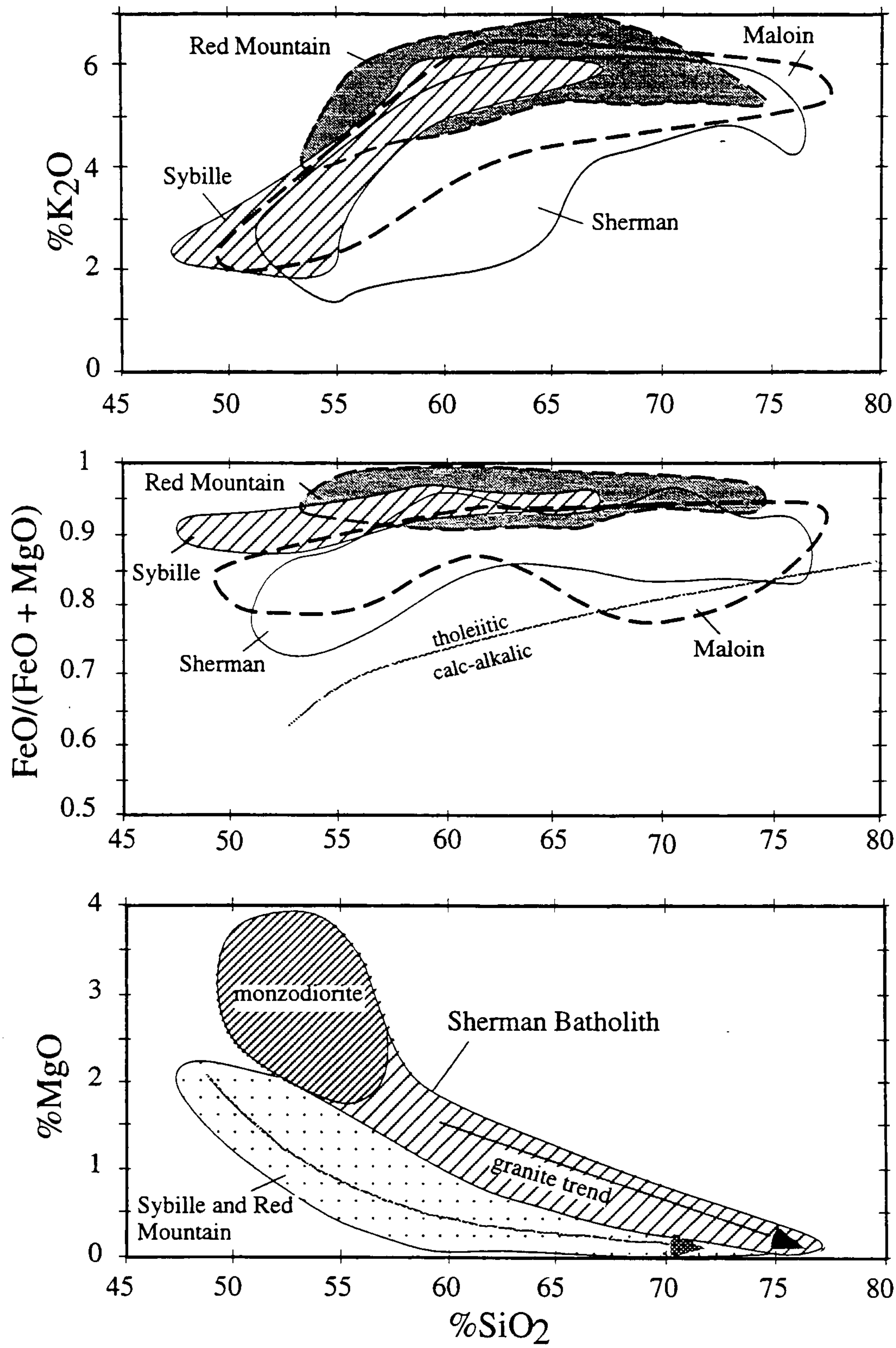


**Figure 10: Comparison of the geochemical trends of the Sherman Granite, Sybille, Maloin, and Red Mountain plutons. Data from Fountain et al. (1981), Kolker and Lindsley (1989), Edwards (1993), and Anderson (1995) and unpublished data of C.D. Frost.**

two major kinds of trends on this diagram (Scoates, 1994). A "normal" differentiation process in which plagioclase and ferromagnesian minerals both evolve, should produce a decrease in both An and Mg# with increasing differentiation, resulting in an array that has a positive slope on this diagram. However, if anorthosite was produced from a diapir that consisted of a large amount of plagioclase and a small amount of residual melt, then the differentiation of plagioclase towards more albitic compositions may be buffered by the huge reservoir of plagioclase in the crystal mush. In such instances, arrays with a vertical or steeply negative slope may result (Raedeke and McCallum, 1980). From Figure 9 we can identify three distinct anorthositic diapirs: 1) Horse Creek anorthosite with an average composition around $An_{60}$, 2) Chugwater anorthosite, with an average composition of $An_{54}$, and 3) the core of the Poe Mountain ALZ diapir with an average composition of $An_{46}$. The LLZ of the Poe Mountain anorthosite has an oblique trend on this diagram that is consistent with co-fractionation of plagioclase and ferromagnesian silicates. This is agrees with the fact that the LLZ is poorer in plagioclase and richer in ferromagnesian silicates that the other plutons in the LAC. The Snow Creek Anorthosite dataset is small, limiting our ability to interpret its trend. It overlaps the fields for Chugwater and Poe Mountain anorthosites on Figure 9.

Rocks of the Sybille, Red Mountain and Maloin Ranch plutons and the Sherman granite batholith exhibit the potassic, iron-enriched compositions typical of the anorogenic granite association (Anderson, 1983) (Figure 10). The Sybille and Red Mountain monzonites and granites have uniformly high FeO*/(FeO* + MgO) of 0.9 or greater, whereas the Maloin and Sherman suites exhibit a trend of increasing iron-enrichment with increasing silica (Figure 10 B). Maloin and Sherman samples have on average lower potash contents than Sybille and Red Mountain samples of comparable $SiO_2$.

On Harker diagrams, the Sybille and Red Mountain analyses produce smooth convex upward curves, consistent with fractional crystallization of olivine, pyroxene and feldspar. The data for the granites of the Sherman batholith are more linear (see for example, MgO versus $SiO_2$; Figure 10 C). Porphyritic granite samples are intermediate between Lincoln and Sherman granite and the most evolved monzodiorite compositions, consistent with an origin by magma mixing (Edwards, 1993; Vasek, 1995). Field evidence of mixing also has been documented from the Maloin Ranch pluton (Kolker and Lindsley, 1989).

## Rare Earth Elements

The REE patterns for the rocks of the LAC have similar LREE enrichments, but different Eu anomalies (Figure 11). The anorthosites have distinct positive Eu anomalies, as do the least differentiated rocks, the high-Al gabbros. The ferrodiorites also have only small negative or small positive Eu-anomalies (Mitchell et al., 1996). It has often been interpreted that ferrodiorite cannot be a residual liquid following crystallization of anorthosite, because it was thought that following extensive crystallization of plagioclase the residual liquid would not have a positive Eu anomaly. However, this argument presumed that the parent magma for the anorthosite complex had no Eu anomaly. Fractionation of plagioclase from a high-Al gabbro with a prominently positive Eu anomaly, such as the high-Al gabbros of the LAC (Mitchell et al, 1995), could produce a residual liquid with only a small negative or slightly positive Eu anomaly.

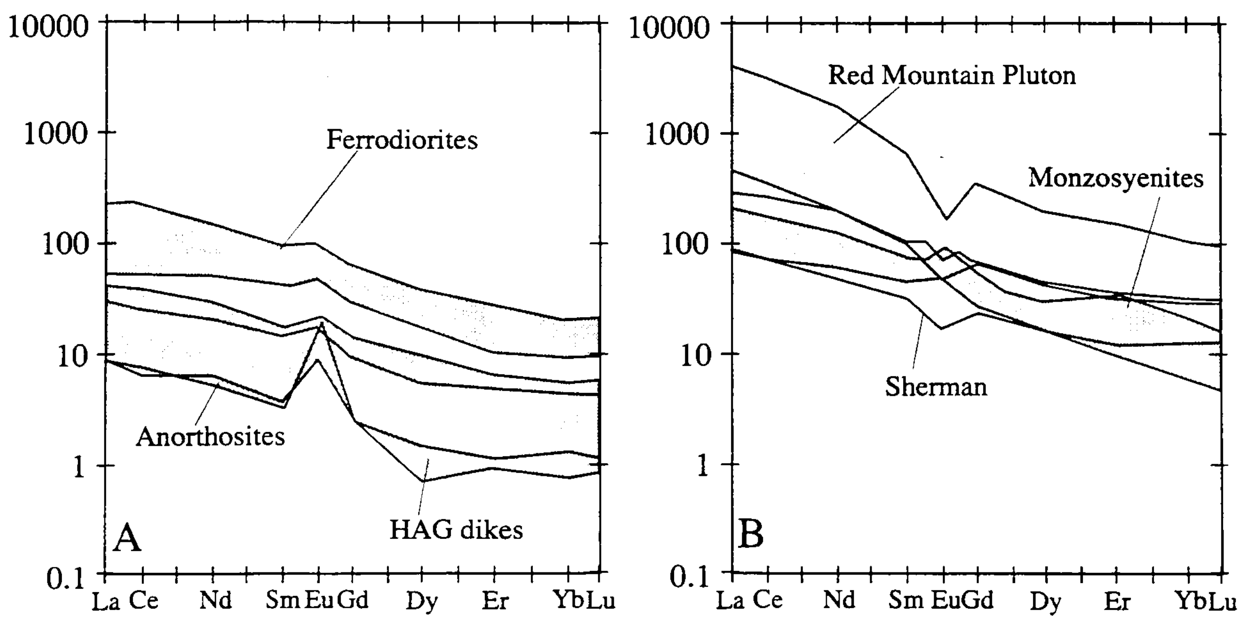


**Figure 11: REE content of rocks from the LAC and Sherman batholith. HAG = high - Al gabbro. Data from Mitchell et al. (1995), Scoates (1994), Anderson (1995) and unpublished data of C.D. Frost.**

REE contents of the monzonitic plutons and the Sherman batholith are higher than the REE contents of LAC anorthosites and high-alumina gabbros, but overlap the REE patterns for the LAC ferrodiorites. Like the ferrodiorites, the Sybille monzosyenites and the Red Mountain fayalite monzonites have positive Eu anomalies, which are produced at least in part by the presence of cumulus feldspar (Fountain et al, 1981; Kolker et al., 1990; Anderson, 1995; Scoates and others, 1996). The more evolved rocks of the Red Mountain pluton and the Sherman batholith have negative Eu anomalies. Data from the Red Mountain pluton suggests that as differentiation proceeds the Eu anomaly changes from slightly positive to moderately negative. The high REE abundances in a number of the Red Mountain monzonites are directly related to the modal abundance of allanite. The Red Mountain granites have lower REE contents, probably reflecting depletion of REEs from the melt by crystallization of zircon and allanite (Anderson, 1995). The youngest granite from the Sherman batholith, the Lincoln granite, has the lowest REE content of the batholith, again reflecting removal of REEs by accessory phases in earlier formed portions of the batholith.

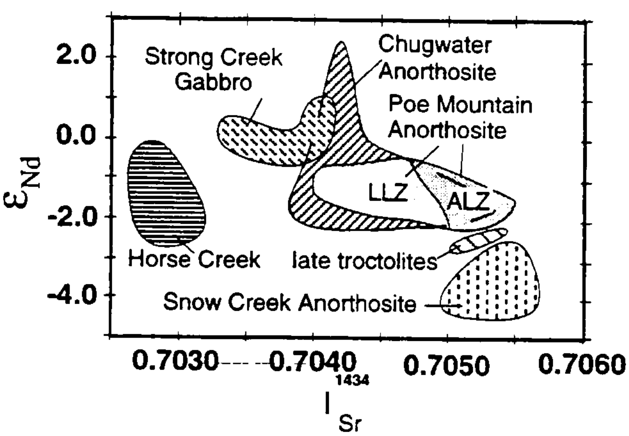


**Figure 12: Initial isotopic composition calculated at 1434 Ma for the various anorthositic plutons in the Laramie Range. Data are from Mitchell et al. (1995), Scoates and Frost (1996), and unpublished data of C.D. Frost.**

## Radiogenic isotopes

The anorthositic intrusions of the Horse Creek and Laramie Anorthosite Complexes have distinctive $\varepsilon_{Nd}$ and $I_{Sr}$ signatures (Figure 12). At the time of its formation (1762 Ga), the Horse Creek Anorthosite had Nd and Sr isotopic compositions that are similar to the contemporary mantle or the juvenile crust into which it was emplaced (C.D. Frost, unpublished data). In contrast, the anorthosites of the Laramie Anorthosite Complex have a higher $I_{Sr}$, indicative of a greater participation of Archean component in these rocks than in the Horse Creek Anorthosite. However each pluton of the LAC is isotopically distinctive (Figure 12).

At 1434 Ma, the Poe Mountain anorthosite had a relatively constant $\varepsilon_{Nd}$ at around -1, but the LLZ and ALZ were clearly distinguished by the strontium isotopes (Scoates and Frost, 1996). The ALZ had a higher $I_{Sr}$ (and slightly lower $\varepsilon_{Nd}$), indicating that it had incorporated slightly more continental material than did the LLZ. Most of the samples of the Chugwater Anorthosite had $I_{Sr}$ similar to that of the LLZ of the Poe Mountain anorthosite ($I_{Sr}$ = 0.7040-0.7045). The Chugwater anorthosite had a wider range in $\varepsilon_{Nd}$ , ranging from -2 to +2. The two samples of the Chugwater anorthosite that had $I_{Sr}$ greater than 0.7050 and that overlap the isotopic composition of the ALZ come from the northernmost limits of the Chugwater anorthosite, adjacent to the ALZ. We interpret their isotopic signature to reflect the fact that they incorporated more Archean crust than did anorthosites further south, which were emplaced into Proterozoic crust. In general the isotopic signatures of the Poe Mountain anorthosite, Chugwater anorthosite, and Strong Creek gabbro indicate a decreasing crustal component in these rocks with decreasing relative age. This suggests that the conduit up which these magmas passed become cleansed of crustal components with time, a trend similar to that observed in modern volcanoes (Myers et al., 1985) (Scoates and Frost, 1996).

The late troctolites that intrude the Chugwater and Poe Mountain anorthosites typically have a lower $\varepsilon_{Nd}$ and higher $I_{Sr}$ than the anorthosites into which they intrude. This indicates either that they were derived from a different magma body than their anorthosite hosts, or that the magma body from which they were derived progressively assimilated crust as it evolved.

The Snow Creek anorthosite also shows evidence of more crustal assimilation than the other plutons in the LAC, even though it appears to be the youngest of the plutons. This relatively high degree of crustal assimilation is consistent with the local occurrence of xenocrystic quartz in the Snow Creek anorthosite, the inherited components in zircon as indicated by the U-Pb systematics, and the absence of magnetite from the paragenesis. This contamination may be related to the geographic position of the Snow Creek anorthosite, which was emplaced to the west of the main conduit of the other anorthosite plutons, and thus encountered crustal components that had not been consumed by previous pulses of magma.

The high-Al gabbros, which are proposed to represent relatively primitive melt that evolved to form the anorthosites, show a wider range of isotopic variation than do the anorthosites (Mitchell et al., 1995). Some have relatively mantle like values for $\varepsilon_{Nd}$ and $I_{Sr}$ (+2 and .7035, respectively), but others show strong evidence of crustal contamination, with values of $\varepsilon_{Nd}$ as low as -5 and of $I_{Sr}$ higher than 0.707. The high-Al gabbros with the higher amounts of crustal components lie in the northern portion of the LAC, where the crust is dominated by Archean rocks. Like the high-Al gabbros, the ferrodiorites show a wide range in $\varepsilon_{Nd}$ and $I_{Sr}$ ($\varepsilon_{Nd}$ ranges from 0.8 to -3.5 and

$I_{Sr}$ from 0.704 to 0.713) (Mitchell et al, 1996). Because this range is far greater than that of the anorthosites, it strongly suggests that the evolution of the magma toward ferrodiorites involved additional degrees of crustal assimilation. Furthermore, the wide range of isotopic signatures indicates that the ferrodiorites in the intrusion did not evolve from a single magma, but that they represent different batches of melt that were variably contaminated with continental crust (Mitchell et al., 1996).

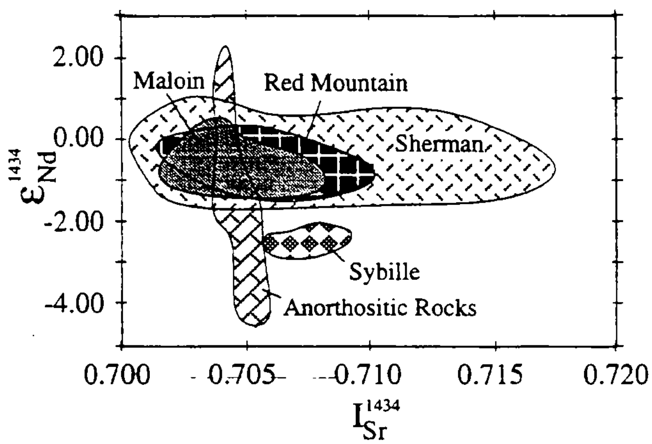


**Figure 13: Diagram comparing the isotopic signature of the monzonitic plutons and the Sherman Batholith. Data from Kolker et al. (1991), Anderson (1995) and unpublished data of C.D. Frost.**

The initial Sr and Nd isotopic composition of the monzonites and granites of the LAC and Sherman batholith form horizontal trends on a diagram of $\varepsilon_{Nd}$ versus $I_{Sr}$ (Figure 13). These horizontal arrays contrast with the near-vertical array formed by the anorthositic rocks of the LAC. These different trends are caused by the differing abundance of Nd and Sr in anorthosite as opposed to monzonite and granite (Geist et al., 1990): the anorthosites have low Nd concentrations, hence even a small amount of contamination with relatively Nd-rich continental crust produces a shift towards more negative $\varepsilon_{Nd}$ values characteristic of Precambrian crust. Moreover, anorthosites have high Sr relative to typical continental crust, therefore contamination has a smaller effect on the Sr isotopic composition of anorthosite than it does on the Nd isotopic composition. The monzonitic rocks have higher Nd and lower Sr, such that assimilation of continental crust produces a horizontal shift on Nd versus Sr isotope diagrams.

The field for Sybille monzosyenites is displaced towards more negative $\varepsilon_{Nd}$ compared to the fields for Maloin and Red Mountain plutons and the Sherman batholith (Figure 13). Scoates et al. (1996) suggested that Sybille magmas were contaminated with Archean continental crust, xenoliths of which are abundant within the pluton. By contrast, the rocks of the Red Mountain pluton, although also emplaced into Archean crust, have less negative $\varepsilon_{Nd}$ values. This younger monzonitic pluton apparently ascended through a conduit that was shielded from Archean crust, perhaps because it passed through slightly older units of the Laramie Anorthosite Complex.

The Maloin Ranch pluton and the Sherman batholith are emplaced into Proterozoic country rocks, although Archean crust probably is present at depth (Allmendinger et al., 1982; Johnson et al., 1984). The Proterozoic gneisses and volcanic rocks have Pb, Nd and Sr isotopic characteristics at 1434 Ma that are indistinguishable from those of the Maloin and Sherman samples, suggesting a possible origin by crustal melting. However, an origin from the mantle, accompanied by assimilation of a small amount of Archean crust, would also be compatible with the observed isotopic compositions.

## EVOLUTION OF THE LAC AND SHERMAN BATHOLITH

The parent magma of the anorthositic rocks probably was of mantle origin. However, the most primitive magmas that we see in the complex are compositionally distinct from typical mantle-derived basalt (Mitchell et al., 1995). Some process must have taken place to enrich the parent melt in Al, Ti, and increase the ratio of Fe to Mg. We accept the model of Longhi et al. (1993) in which anorthosites form in two stages, first an early crystallization of basaltic melt produced by partial melting of the mantle melt near the base of the crust and second, a rise of these plagioclase-saturated magmas to middle crustal levels where the anorthosites were emplaced. Evidence of an earlier, deep-level magma chamber is seen in high-Al pyroxenes found locally in the LAC (Scoates, 1994), similar to those reported from other massif anorthosites (Emslie, 1975; Morse, 1975; Dymek and Gromet, 1984). A clinopyroxene megacryst from the Poe Mountain anorthosite is in strong isotopic disequilibrium with the enveloping anorthositic cumulates and its $Cr/Al_2O_3$ ratio indicates that it may have crystallized at pressures above 10 kilobars (c.f. Fram and Longhi, 1992).

The oldest rocks in the LAC that are preserved are leucogabbros that now occur as blocks within the upper portion of the Poe Mountain anorthosite (Scoates, 1994). It is unclear whether these record the presence of a pluton that existed at this level prior to the intrusion of the Poe Mountain anorthosite, or whether they were rafted in from depth during the emplacement of the Poe Mountain anorthosite. Additional fragments of an early leucogabbro intrusion also occur as inclusions in the northern part of the Sybille pluton. These are either portions of this early leucogabbro or a dismembered roof to the Poe Mountain anorthosite. The Poe Mountain anorthosite represents either the layered cumulates that formed at the base of this intrusion, or a later intrusion into the leucogabbro. The cumulates probably formed on the intrusion floor that was either flat or gently sloping (Figure 14 A). Intrusion of the Chugwater anorthosite and possibly even the core anorthosites of Poe Mountain anorthosite deformed the cumulates of the Poe Mountain anorthosite into a broad dome (Figure 14B). This doming probably occurred when there was still melt in the Poe Mountain magma chamber, as indicated by the abundant slump structures seen in the Poe Mountain anorthosite, by the decrease in deformation intensity as one moves stratigraphically upward in the pluton (Scoates, 1994), and by the fact that the deformation occurred largely by grain boundary migration, a process that is most effective if there is a melt present to flux the migration (Lafrance et al., 1996).

The relationship between the various portions of the Chugwater anorthosite is poorly understood. The eastern portion, the Coyote Flat dome (Figure 3), is more intensely deformed than the rest of the intrusion.

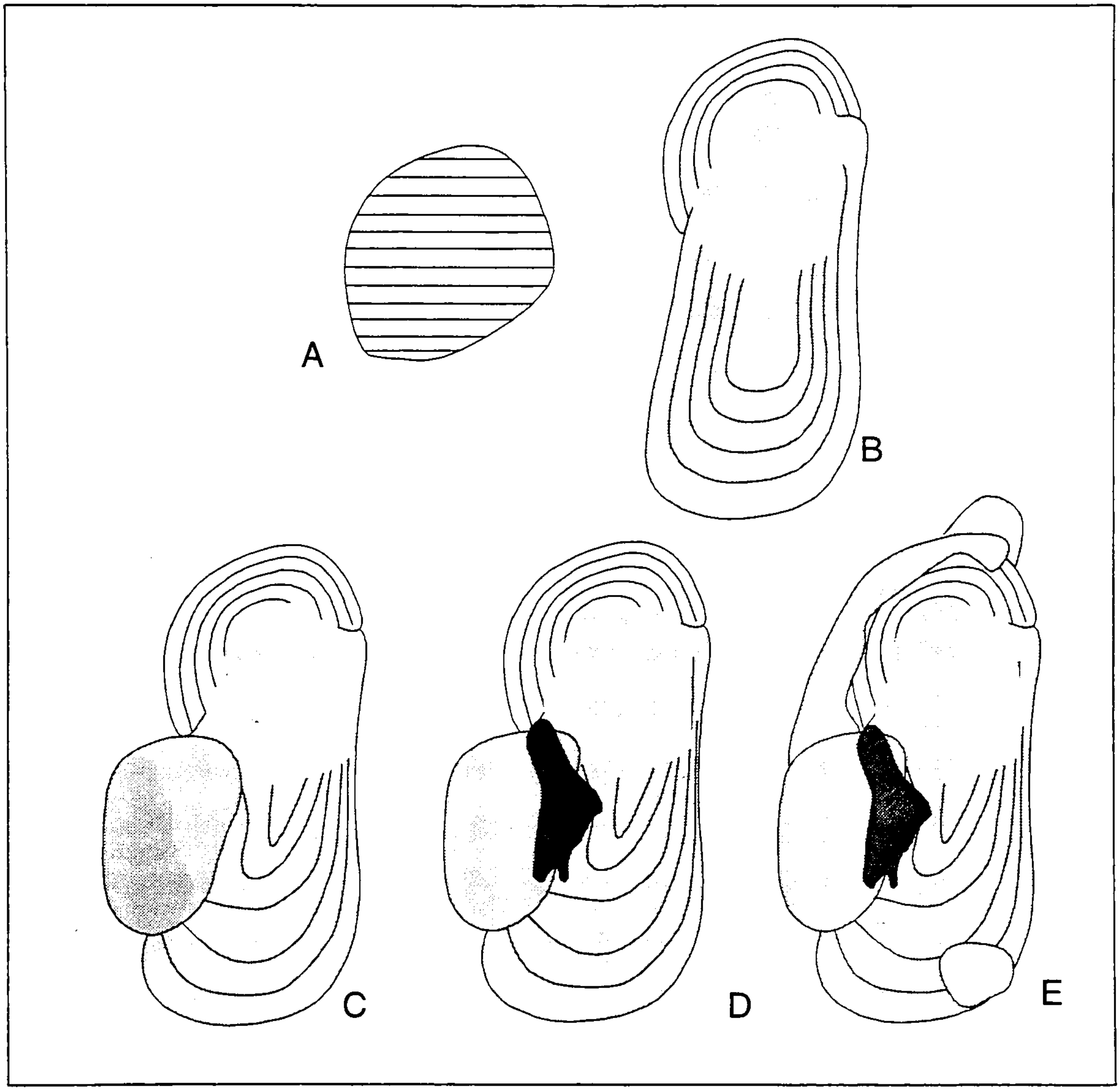


**Figure 14: Schematic model for the evolution of the Laramie Anorthosite Complex. A. Emplacement of the Poe Mountain Anorthosite cumulates. B. Doming of the Poe Mountain cumulates by intrusion of the Chugwater anorthosite and possibly by intrusions of the Poe Mountain core anorthosites. C. Emplacement of the Snow Creek anorthosite causing the deformation of the Chugwater anorthosite. D. Emplacement of the Strong Creek gabbro between Snow Creek and Chugwater anorthosites. E. Emplacement of the Sybille, Red Mountain, and Maloin plutons.**

However, the rocks that occur within it are chemically and isotopically identical to the rest of the Chugwater anorthosite. We conclude, therefore, that the Coyote Flat dome is an earlier portion of the Chugwater anorthosite that was intruded and deformed during the intrusion of the main stage Chugwater and we do not show it as a separate unit on Figure 14. The Snow Creek anorthosite was emplaced shortly after the Chugwater anorthosite. It truncated layers in the upper Chugwater anorthosite and deformed the foliation in the core (Figure 14 C). By the time that the Greaser intrusion and Strong Creek gabbro, the last of the mafic portions of the LAC, were emplaced, most of the high-temperature deformation within the LAC had ceased. Both intrusions seem to have been emplaced along the contact between the Snow Creek anorthosite and the Chugwater anorthosite (Figure 14 D). It is possible that there was still melt present in the Chugwater anorthosite at the time the Strong Creek gabbro was intruded, since some mafic layers can be traced from the core of the Chugwater anorthosite into the southern portion of the Strong Creek Gabbro. Along the northern contact of the Strong Creek it appears to have been emplaced by stoping, for here it is riddled with inclusions of anorthosite. This disruption of earlier rocks has made it difficult to determine in this region the exact limits of the Poe Mountain, Chugwater, and Snow Creek anorthosites.

Following the emplacement of the Strong Creek gabbro, monzonitic and syenitic plutons were intruded between the LAC and the surrounding country rock. The Sybille pluton was emplaced first on the north, followed by the Red Mountain pluton. At approximately the same time, the Maloin Ranch pluton intruded on the southeastern margin of the Chugwater anorthosite. Scoates et al. (1996) have suggested that the parent magma for Sybille monzosyenite is a ferrodiorite. Ferrodiorite dikes and pods within the anorthositic rocks of the LAC are interpreted as residual magmas expelled from anorthositic cumulates late in the magmatic history of these plutons (Mitchell et al., 1996), and thus are known to have been present at the time of Sybille magmatism. Continued fractionation of ferrodiorite follows a path experimentally determined by Lindsley (in prep) that upon 90% crystallization approaches the major element composition of Sybille monzosyenites. Addition of alkali feldspar produces the major and rare earth characteristics of Sybille samples. Modest amounts of crustal assimilation are evident in some samples. According to this model, monzosyenites are co-magmatic with residual magmas from anorthosite formation, but they require extensive fractional crystallization to acquire their extremely potassic, iron-enriched compositions.

The model developed for the Sybille pluton may be applicable to the Red Mountain and Maloin Ranch plutons as well. However, it is unlikely to account for the extensive exposures of granite present in the Sherman batholith. There is no gravity anomaly beneath the Sherman batholith that may be attributed to dense ferrodioritic cumulates, as there is beneath Sybille. Moreover, the Sherman batholith extends far south of the anorthosite plutons, where there is no evidence for large volumes of ferrodiorite that are required by the Scoates et al. (1996) model. Hence the origin of the Sherman batholith is enigmatic, because geochemical and isotopic data cannot discriminate between mantle and crustal sources.

## TECTONIC SETTING OF THE PROTEROZOIC PLUTONISM IN THE LARAMIE MOUNTAINS

In the preceding discussion we have described two anorthosite complexes, the 1.76 Ga Horse Creek Anorthosite Complex, and the 1.43 Ga Laramie Anorthosite Complex, both emplaced along the Cheyenne belt between the Archean Wyoming province and the Proterozoic Colorado province. Collision of Proterozoic island arc terranes with the Wyoming craton occurred between approximately 1780 and 1760 Ma (Karlstrom and Houston, 1984; Houston et al., 1989; Premo and Van Schmus, 1989; Resor, 1996; and Chamberlain, unpublished data). The 1.76 Ga age of the Horse Creek complex is correlative with the timing of the last movement along the Cheyenne belt, which has been interpreted to be a dextral strike-slip motion (Duebendorfer and Houston, 1987). We propose that the HCAC was generated in a zone of transtension related to dextral shearing during the late stages of arc-continent collision. This pre-existing zone of crustal weakness may have been reactivated approximately 330 m.y. later and led to the development of renewed anorthositic and granitic magmatism evidenced by the 1.43 LAC and Sherman batholith.

## ROAD LOG

**Note:** Many of the stops discussed below occur on private land. Anyone planning to use this guide for future trips must make sure that landowner permission has been obtained.

### Day 1: Horse Creek and Laramie anorthosites

| total mileage | mileage between points | |
|---|---|---|
| 0.0 | 0.0 | Intersection of Ninth St. and Lewis St. in Laramie. Drive North on Ninth St. |
| 0.7 | 0.7 | Intersection with Reynolds St. |
| 1.4 | 0.7 | Northern city limits of Laramie, Ninth St. becomes Albany County road 17. Road climbs slope consisting of red-weathering Triassic Chugwater Formation. |
| 6.4 | 5.0 | Round the northern extension of The Spur, a north-west plunging anticline in the Pennsylvanian-Permian Casper Formation. |

9.2 2.8 Enter Rogers Canyon, the low cliffs on each side of the road are formed by limestone layers in the Casper Formation.

10.5 1.3 Pavement ends.

10.8 0.3 Crest of the Laramie Range, slopes on either side of the road are underlain by red sandstones of the upper Pennsylvanian Fountain Formation.

11.3 0.5 Unconformity between Paleozoic rocks and the Horse Creek anorthosite.

11.7 0.4 Small pits to the right are prospects dug into the Horse Creek anorthosite by ALCOA as prospects for aluminum.

13.1 1.4 Cross cattle guard and stop on right side of the road, walk across the road to low outcrops of anorthosite.

**Stop 1.1: Horse Creek Anorthosite.** At this stop we will see a typical exposure of the Horse Creek anorthosite. The HCa differs from the anorthosite from the Laramie Anorthosite Complex to the north in that it has been metamorphosed. Most of the ferromagnesian minerals have been converted to hornblende, actinolite, and chlorite and plagioclase commonly has a distinct lavender color due to growth of small grains of epidote or clinozoisite. The metamorphism was largely a static hydration event, since primary magmatic layering can be found in many places throughout the HCa.

Continue east on Co. Rd 17 across the Horse Creek anorthosite.

14.6 1.5 Cross Schoolhouse Creek.

16.0 1.4 Tailings of Strong Mine on the east side of the road. The Strong Mine is a copper mine that was developed in the early years of the 20$^{th}$ century. It was served by the town of Leslie, which has since disappeared without a trace. The mine was after ore that was hosted in diorite and gabbro dikes cutting the anorthosite. Along with copper, the ore contained significant amounts of gold, silver, and tungsten. The mine was reopened briefly during World War II for the tungsten.

16.6 0.6 Cross Horse Creek.

17.2 0.6 Magmatic layering dipping southeast can be seen on the low hills southeast of the road.

19.6 2.4 The hogbacks of Casper Formation appear ahead, marking the eastern margin of the Laramie Range. The ridge behind the hogbacks is held up by the Oligocene-Miocene Arikeree Formation and marks the edge of the Tertiary on-lap in the area.

20.7 1.1 Cross onto hornfelses in the complex contact zone. This belt runs approximately NE-SW. The prominent nose on the southern horizon is underlain by quartzite that is part of this contact aureole.

21.1 0.4 First appearance of Sherman granite as outcrops on either side of road. We will look in detail at the Sherman batholith on Day 3.

22.0 0.9 Cross another ridge held up by hornfels and anorthosite.

22.2 0.2 Cross back into Sherman granite.

25.2 3.0 Road turns north and runs parallel to the frontal thrust. Park alongside road for a photo opportunity.

**Stop 1.2: Frontal Thrust of the Laramie Range.** This stop provides an opportunity to photograph the Laramide thrust that forms the eastern edge of the Laramie Range. The hills to the east are underlain by gray limestones of the Casper Formation and (Pennsylvanian-Permian) and redbeds of the Chugwater (Triassic) Formations. The beds are dipping away from us with the Chugwater beneath the Casper; clearly they are overturned. The trace of the fault can be seen climbing the hill to the south of us. Continue east on the road.

25.7 0.5 Cross the frontal thrust of the Laramie Range.

26.0 0.3 View north toward complex structure on the footwall of the thrust.

28.5 2.5 Horse Creek, Wyoming, turn left off Wyoming Highway 211. As we drive north we are driving along the Eocene-Oligocene White River Formation, which here laps over onto the deformed rocks at the front of the Laramie Range. To the right are white cliffs of the Oligocene-Miocene Arikaree Formation.

32.6 4.1 Crest of hill. To the north we can see the Casper Formation dipping toward us off of unnamed hills. Locally in the valley you can see red rocks of the Chugwater Formation.

37.3 4.7 Turn right at sign pointing toward Iron Mountain.

38.4 1.1 Farthing (Iron Mountain Post Office), Wyoming, turn left on Farthing Ranch road and drive across low meadows toward the Laramie Range.

39.7 1.3 Ranch House of Farthing Ranch. Continue west on private ranch road toward Laramie Range.

40.0 0.3 Cross South Chugwater Creek.

43.1 3.1 Cross the frontal range thrust. Here the thrust is buried under Tertiary deposits. Begin climbing on slopes underlain by rocks of the Chugwater anorthosite of the Laramie Anorthosite Complex.

44.6 1.5 Pass two large granitic dikes at the crest of the hill. Between here and Shanton Creek the Chugwater anorthosite is cut by many granitic dikes. Adjacent to the dikes, the primary pyroxenes and olivines in the anorthosite have been hydrated to hornblende. Despite the fact that it is cut by local intense deformation zones that are not present further west, we map this as part of the Chugwater Anorthosite, because it is compositionally similar to other portions of the Chugwater Anorthosite and because it has the same U-Pb zircon age.

46.4 1.8 Cross Shanton Creek.

47.8 1.4 Turn left onto dirt track to Shanton mine and bear left at first intersection.

48.0 0.2 Park where the road disappears under tailings.

**Stop 1.3: Shanton Mine**. The Shanton mine is one of the many massive Fe-Ti oxide deposits that dot the LAC. The deposit originally consisted of five small ore bodies that consist almost entirely of magnetite and ilmenite (Fig. 15). The northern most bodies are sub-rounded in shape, while the southern ones are dike-like in morphology. Drilling by the US Bureau of Mines (Hild, 1953) shows that the largest body did not extend to great depth. In 1959, Union Pacific mined several thousand tons of ore for a study of the feasibility of mining. This mining activity, plus the reclamation activity in the late 1980's pretty much destroyed the largest ore body. The two southern bodies are tabular, being 15-30 feet wide, up to 300 feet long and extend up to 300 feet in depth.

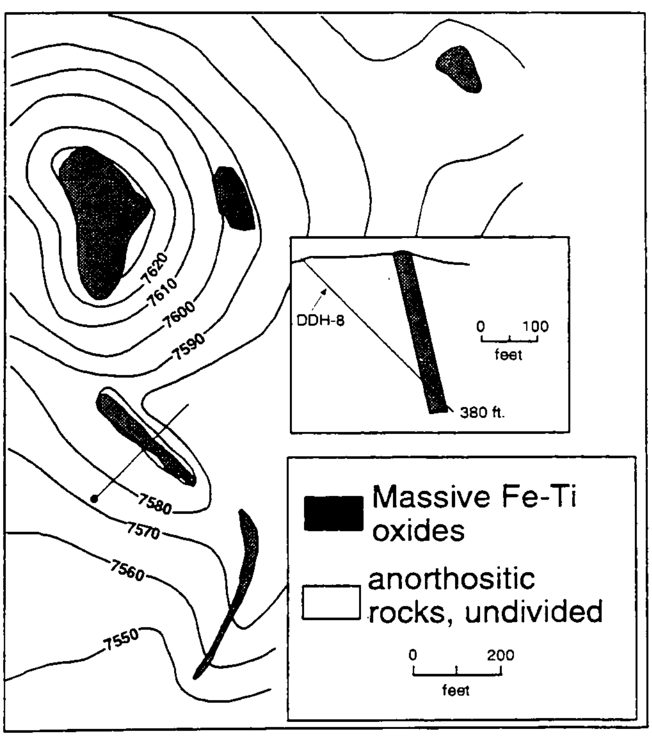


**Figure 15: Geologic relations of the Shanton Mine prior to mining and reclamation; after Hild (1953). Inset shows a cross section parallel to the trend of DDH-8, emphasizing the dike-like shape of the southern oxide bodies.**

Turn around and return to Farthing Ranch road.

48.2 0.2 Farthing Ranch road, turn left.

48.3 0.1 Stop just east of cattle guard and walk to low outcrops north of the road.

**Stop 1.4: Megacrystic Chugwater Anorthosite.** This is a typical outcrop of the Chugwater anorthosite. It consists of megacrysts of plagioclase (about $An_{52}$) that range up to 4 cm in maximum dimension. The megacrysts clearly have undergone high-temperature deformation, as seen by the warped the (010) cleavage surfaces. The original margins of the megacrysts have been modified by neoblastic plagioclase growth that probably occurred at near-magmatic temperatures. Iridescent blue plagioclase can be found locally.

Continue west on Farthing Ranch Road.

49.7 1.4 Crest of hill. Smooth, tree-covered mountains to the west are underlain by Permian Casper Formation that is dipping westward away from us. The more ragged mountains to the northwest are known as the Buttes and are underlain by a septum of granite that lies between the Snow Creek anorthosite and the Greaser intrusion.

51.9 2.2 Stop just north of a culvert over a small tributary to Middle Chugwater Creek and walk west 100 yards to where fresh samples of ferrodiorite have been exposed during construction of a pipeline.

**Stop 1.5: Dike of Ferrodiorite** Ferrodiorite and monzodiorite from dike cutting anorthosite. This dike consists of monzodiorite with angular to rounded blocks of ferrodiorite. We believe that the ferrodiorite was intruded first and that monzodiorite was intruded later and incorporated fragments of the earlier ferrodiorite.

Continue north on Farthing Ranch road.

52.2 0.3 In this area of poor outcrop, we cross over to leucogabbros and leucotroctolites of the Strong Creek Complex, a suite of gabbros and troctolites that intruded into the Chugwater, Poe Mountain, and apparently Snow Creek anorthosites.

52.6 0.4 Cross cattle guard and leave Farthing Ranch.

53.0 0.4 Cross Middle Fork Chugwater Creek.

53.5 0.5 Cross over to gabbros and ferrodiorites of the Greaser intrusion. This intrusion, which forms the rounded brown outcrops that run along the road for the next several miles, has been intruded into the Strong Creek gabbro.

55.2 1.7 Pass entrance to Strong Creek Ranch.

56.6 1.4 Cross back into the Strong Creek gabbro. There are few outcrops in this area, but many prospects attest to the high Fe-Ti oxide content of these rocks.

58.0 1.4 Intersection with Albany County Highway 12. End of private road. Turn right. For the next five miles the road travels across an upland underlain by strongly recrystallized rocks of the Chugwater anorthosite.

59.2 1.2 Iron Mountain haul road exits to the right. This road was built in the 1960s to allow access to the prospect pit at Iron Mountain, which lies about five miles to the east. Iron Mountain is a deposit of iron-titanium oxides that was actively mined for heavy aggregate in the 1960s. Petrologically, it is similar to the Sybille Pit, which we will see on Day 2.

62.8 3.6 Continue to high point on the road and pull over to the right for a photo opportunity.

**Stop 1.6: Overview of the northern Laramie Anorthosite Complex:** This point provides a panorama of the northern part of the Laramie Anorthosite Complex. The tree-covered mountains on the skyline are underlain by Archean granite and granite gneiss. The low topography of the North Fork of Sybille Creek lies between us and these mountains. This area of subdued topography is underlain by the Sybille monzosyenite and is characterized by the rusty color of its soil. Two distinct barren mountains lie to the north. The peak to the left with a fringe of trees is Poe Mountain, which is underlain by the northern most anorthosite pluton, the Poe Mountain anorthosite. The rocky mountain to the right is Red Mountain, the type locality of the Red Mountain pluton. To the right of Red Mountain is tree-covered Squaw Rock, which is underlain by 2.6 Ga. granitic rocks. Far to the east are ridges capped by limestone of the Casper Formation, which has been thrust northward over Archean gneiss.

64.2 1.4 Continue north on Albany Co. 12. and stop on a right hand bend where road construction has exposed fresh Chugwater anorthosite.

**Stop 1.7: Chugwater anorthosite.** This is a good location to collect the Chugwater anorthosite. At this locality the megacrysts are not as abundant as they were at stop 1.3. As at stop 1.3 the plagioclase may be iridescent. There is also a slightly higher concentration of olivine and pyroxene here than at stop 1.3. Also present at this locality is high-aluminum gabbro, which forms a dike running south from the road.

Continue north east on Albany Co. 12.

65.8 1.6 Timber Canyon Ranch road.

66.2 0.4 Here the road drops into the valley of Grant Creek fault. This is a Laramide fault that runs south from Poe Mountain and joins the frontal thrust somewhere south of Iron Mountain. Near Iron Mountain the fault is a west-dipping thrust, but from here north it is a high-angle reverse fault along which displacement slowly dies out to the north. Rubbly pale green outcrops on the right of the road here and elsewhere along this valley (at miles 66.6, 66.9, 68.4, 68.9, 69.5, 70.4, 71.4, 71.9) mark anorthosite gouge developed along the fault. The road follows the trace of this fault for the next five miles.

66.8 0.6 Entrance to the Double J ranch.

74.4 7.6 Intersection with Wyoming 34, turn left and follow the highway west through the canyon of North Fork Sybille Creek. For the next 5 miles the canyon follows the trace of the Sybille fault, a Laramide fault with about 300 meters right-lateral strike-slip displacement.

77.1 2.7 Johnson Creek Road intersects from the left.

77.8 0.7 Stop on the south side of the road at a rest area maintained by the Sybille Game and Fish Experimental Unit and walk west about 100 yards down the highway to a road cut on the north side of Wyoming 34.

**Stop 1.8: Mottled Anorthosite of the Poe Mountain Anorthosite:** This is typical of rocks of the Anorthositic Layered Zone (ALZ), the lower portion of the Poe Mountain anorthosite. The following features may be seen in this outcrop: mafic oikocrysts, layer disruption, an exotic block, a zone on intense recrystallization developed during deformation at near magmatic conditions, and a high-T mylonite zone.

The broad-scale stratigraphy of this locality is made up of two prominent macro-layers. The stratigraphically lower layer is the mottled anorthosite and above this is an anorthosite that contains only rare, fine mafic oikocrysts and is dominated by podiform, coarse mafic clots that are elongate parallel to the overall layering of the outcrop. In both layers the rock has a definite planar fabric that is produced by the orientation of tabular plagioclase, the flattening of the mafic spots, and gross lithologic differences. The dominent oikocrysts are olivine with lesser amounts of Fe-Ti oxide.

The mottles or spots consist of minute plagioclase laths within aggregates of ferromagnesian minerals. These plagioclase chadacrysts randomly oriented and are much smaller than the surrounding plagioclase matrix. The plagioclase in the matrix consists of laths that average 2.3 cm in length. The margins of these laths consist of fine-grained aggregates of neoblastic plagioclase. This is a common texture that is found throughout the Laramie Anorthosite Complex. Lafrance et al. (1996) conclude that this deformation took place due to grain boundary migration and that it probably occurred after a cumulate framework had been established, but before the melt had been entirely expelled from the rock.

Towards the eastern end of the outcrop there is evidence for layer disruption. Here a single prominent mafic layer undergoes a significant amount of downward warping associated with a thickening of the layer.

Plagioclase lamination in the surrounding anorthositic layers follows the trace of the disrupted mafic layer.

At the west end of the outcrop block of medium-grained biotite-bearing olivine leucogabbro appears to have truncated and warped downward a mafic anorthosite layer beneath it. Plagioclase lamination in the anorthosite beneath the mafic layer is also significantly curved. The planar fabric in the leucogabbro is clearly discordant to the outcrop-scale structures. The upper contact of the block is coincident with a strong mylonite that is up to 7 cm. wide in which both the pyroxenes and the plagioclase in the rock were recrystallized. This high-temperature mylonite continues into the anorthositic layer and dies out within a few meters. The deformation style in this mylonite differs strongly from the deformation seen elsewhere in the outcrop and probably represents deformation that took place when melt was no longer present. Such post-magmatic high-temperature mylonites occur locally throughout the complex but they seldom can be traced over a distance of more than a few tens of meters.

Return to cars and continue west on Wyoming 34.

78.4 0.6 Pull off on right side of road just short of the headquarters of Sybille Game and Fish Experimental Unit. Walk about 100 yards east on road toward road cut on north side of road.

**Stop 1.9: Magmatic block and disrupted layering in the ALZ:** This outcrop contains a mixture of podiform pegmatoids, disrupted anorthosite layers, finer-grained gabbroic anorthosite patches, and an exotic block of olivine leucogabbro. The podiform pegmatoids range in composition from anorthosite to olivine leuconorite. Plagioclase grains within the pods may locally exceed 50 cm in length. Contacts with the anorthosite are typicaly gradational. While on a detailed scale the pods tend to anastomose, they are generally conformable to the large-scale igneous structure of the outcrop. Many of the discrete lensoidal mafic pods are not pegmatoidal but appear to be isolated patches of gabbroic anorthosite. Because they differ significantly from the pegmatoids and appear to be broadly stratiform, they are interpreted as dismembered remnants of igneous layering.

Towards the west end of the outcrop is a 10 meter-long block of olivine leucogabbro that has a prominent fabric characterized by the alignment of blebby mafic minerals. This fabric is highly discordant to the gross-scale structures of the anorthosite that surrounds it. The plagioclase lamination at the base of the block conforms to the shape of the block and the layers beneath the block appear to have been extensively disrupted.

Continue west on Wyoming 34.

78.9 0.5 Pull over on a wide area on the south side of the road and walk west along the highway about 100 meters to a cliffy outcrop that is graced in the middle by an obvious slide block. As you walk to the outcrop note how well the layering is exposed on the cliff.

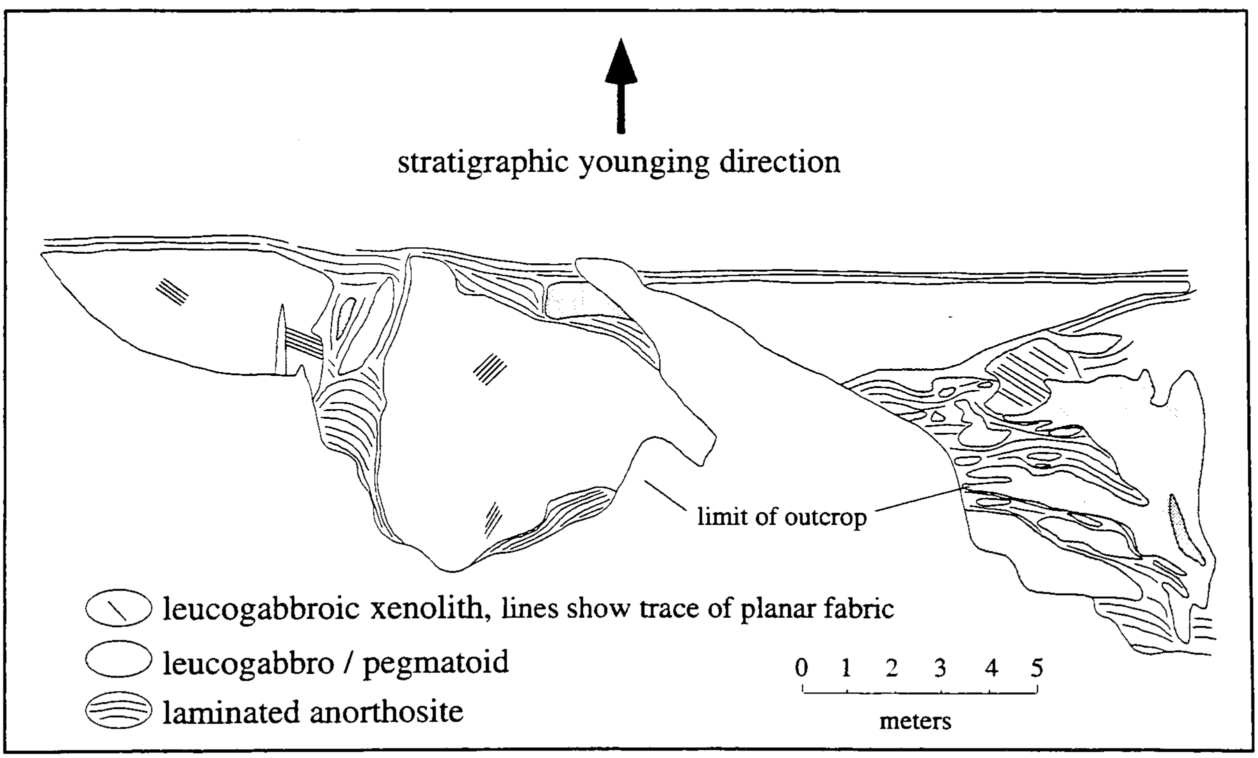


**Figure 16. Detailed sketch of relations at stop 1.10.**

**Stop 1.10: Magmatic features within the ALZ of the Poe Mountain Anorthosite:** This outcrop is dominated by a large rockslide that fell off the cliff in the winter of 1986-1987. Not only did the slide expose some critical textures in the Poe Mountain anorthosite, it also destroyed a fence that had limited our access to the higher areas of the outcrop. The largest block in the rock slide exposes a spectacular example of magmatic layering. Plagioclase is present as megacrysts (crystals up to 11 cm in length), laths 2-6 cm in length and as fine neoblastic grains. Layering is defined by both gradations in plagioclase grain size and, more prominently by variations in the abundance of mafic clots that are similar to the clots seen at stop 1.8.

The main outcrop above the slide blocks displays a series of intriguing relationships (Figure 16). As you approached the outcrop from the vans you will have noticed a very prominent contact at the level of the fence. In general this contact is stratiform and comparable to other meso-scale features higher up the cliff face. However, careful observation reveals this to be upper contact of several distinct blocks. All blocks are medium-grained olivine leucogabbro and most contain a prominent fabric that is defined by the orientation of blebby mafic minerals and which lies at high angles to the general layering of the area. Along the margins of each block there is a sheath of plagioclase laths that conforms to the general shape of the block. Above the blocks the lamination is conformable to the large-scale structures indicating that the stratigraphic up position is upward. Immediately above the anorthosite layer capping the disrupted zone is a zone dominated by plagioclase that has grown perpendicular to the contact. Single grains commonly are 1 m in length and only a few centimeters wide. The largest crystals we have found measures 218 cm x 1.8 cm. Local pockets of quartz and calcite, commonly rimmed by greenish alteration (mostly prehnite, some pumpellyite) alteration in the plagioclase may be locally observed.

| | | |
|---|---|---|
| | | Continue east along Wyoming 34 . |
| 81.7 | | Pull-off on the north side of the highway. Park the cars and walk east to a large road cut. |

**Stop 1.11: Medium-scaled layering in leucogabbro.** This is a good example of the layering found in the LLZ. The contact between the LLZ and the ALZ lies several hundred meters to the east of us. The orientation of the layering here is nearly north-south and dips to the west. Modal layering predominates here, produced largely by differences in the relative abundances of ferromagnesian minerals and plagioclase. In many respects textures here resemble those seen at stop 1.8, with the mafic minerals forming clots surrounding poorly oriented plagioclase. The rock here also has greenish spots consisting of muscovite, calcite, and prehnite, which probably formed from late deuteric fluids. High on the eastern edge of the outcrop are irregularities in the layering that we interpret as having been produced by slumping.

| | | |
|---|---|---|
| | | Continue on Wyoming 34. |
| 82.6 | 0.9 | Contact between Poe Mountain anorthosite and the Sybille pluton. The rocky peak to the right is Sheep Rock and is composed of granophyric granite, which probably represents partial melts of the granitic country rock produced during the emplacement of the LAC. The next five miles the route passes through various units of the Sybille pluton. We will stop at exposures of this rock during Day 2 of the field trip. |
| 87.8 | 5.2 | Contact with Archean granites. The hills in front and to the right are held up by Archean granitic gneiss that is cut by numerous dikes of diabase that have been various metamorphosed in amphibolite facies. The dikes are probably part of a 2.01 Ga dike swarm and, outside of the contact aureole, they have been metamorphosed at 1.76 when rocks of the Colorado province were thrust onto the Wyoming province. |
| 89.2 | 1.4 | Morton Pass. This marks the unconformity between the Casper Formation and the Archean gneiss. |
| 91.4 | 2.2 | Albany Co. Road 12 enters from left. |
| 102.1 | 10.7 | Intersection with US 30/287. Turn left and continue to Laramie. |
| 118.8 | 16.7 | Intersection of US 30/287 with Curtis Street at northern limits of Laramie. |

## Day 2: Sybille Pluton and its Contact Aureole

| total mileage | mileage between points | |
|---|---|---|
| 0.0 | 0.0 | Intersection of US30/287 and Curtis Street at northern limits of Laramie. |
| 0.1 | 0.1 | Low bluffs of red shales and sandstone are part of the Triassic Chugwater Formation. The smooth ridges on the right are a dip-slope in the Permian-Pennsylvanian Casper Formation. |
| 16.7 | 16.6 | Intersection with Wyoming 34, turn right. |
| 27.4 | 10.7 | Intersection with Albany County Road 12. |
| 29.6 | 2.2 | Morton Pass, cross the unconformity between the Casper Formation and the Archean granite gneisses. Archean gneisses here are cut by numerous metamorphosed diabase dikes that were emplaced at 2.01 Ga. |
| 31.0 | 1.4 | Contact between the Sybille pluton and Archean gneisses. |
| 36.2 | 5.2 | Contact between the Sybille pluton and Poe Mountain anorthosite. |
| 41.7 | 5.5 | Intersection with Johnson Creek Road. |
| 42.0 | 0.3 | Intersection with track leading to the Sybille Pit. Drive through gate and continue up private road to the pit. |
| 42.5 | 0.5 | Sybille Pit. |

**Stop 2.1: Sybille Pit.** On the skyline to the east is a good view of Sheep Mountain, a klippe of Casper Formation that lies upon Archean granite gneisses. These gneisses are intruded by the Mule Creek lobe of the Sherman batholith. The Precambrian rocks are cut by the Wheatland fault, a normal fault that has down-dropped the northern block. Although the fault may have a Laramide component, it locally cuts Tertiary rocks, indicating that it has had recent motion.

To the west is a prospect pit that was dug into a small Fe-Ti oxide deposit in the 1950's to provide heavy aggregate. The Fe-Ti oxides are intimately associated with a leucotroctolite that is intruded into the ALZ of the Poe Mountain anorthosite. Fe-Ti oxides are concentrated on the lower stratigraphic horizons of the pit. The Fe-Ti oxide body contains 34 - 99% Fe-Ti oxides, up to 10% olivine ($Fa_{50-60}$), up to 50% apatite, and minor plagioclase ($An_{46-98}$), augite, hercynite, and graphite. The host troctolite contains olivine ($Fa_{60}$) plagioclase ($Ab_{53}An_{45}Or_2$), apatite, plus minor augite, inverted pigeonite, and oxides.

At the back of the pit are numerous fine-grained, brown-weathering blocks that were bulldozed down to this level when the pit was "reclaimed" in the mid '80s. These rocks come from a distinctive composite dike that we have been able to trace for more than 4 miles. The host of the dike is a syenite or monzosyenite, consisting of greasy-green alkali feldspar and fayalite - an assemblage very similar to that found in the Sybille Monzosyenite. Incorporated in this host is a fine monzodiorite dike that shows ample evidence of having been chilled against the host monzosyenite. We interpret the monzodiorite as being a residual liquid from the anorthosite that was intruded into a monzosyenite dike at the time when the magma in the dike was still liquid. The latest magmatic event was the emplacement of granitic dikes, which locally hydrated the anorthosite and troctolite into which they were intruded.

| | | |
|---|---|---|
| 42.6 | 0.1 | After examining this outcrop, walk down the road 0.1 miles to a weathered outcrop on the right side of the road. |

**Stop 2.2: High-Al Augite.** This rough-looking outcrop is a raft of coarse-grained plagioclase and augite. The augite from this locality has a Mg/(Fe+Mg) ratio of 0.681 and its reconstructed composition contains 6.2 weight % $Al_2O_3$. The augite has exsolved plagioclase + olivine and these can be seen in hand specimens as fine lamallae. High pressure fixes Al in pyroxene and Al content of the pyroxene from this iocality is consistent with equilibration at 13 kilobars (Fram and Longhi, 1992).

| | | |
|---|---|---|
| | | Return to vehicles and continue down road to Wyoming 34. |
| 43.0 | 0.4 | Turn left onto Wyoming 34, be sure to close the gate! |
| 48.8 | 5.8 | Contact between Sybille pluton and Poe Mountain anorthosite. |
| 48.9 | 0.1 | Pull off on wide area to left of the road adjacent to a red barn. Cross the road to an outcrop on the north side of the highway. |

**Stop 2.3: Monzodiorite.** The dike at this outcrop is a fine monzonite with the mineral assemblage olivine($Fa_{82}$) - orthopyroxene - pigeonite - augite - magneitte - ilmenite - plagioclase($An_{27}$). Rocks like this usually occur as fine-grained margins to or inclusions within the Sybille Monzosyenite. They also form dikes intruding the anorthositic rocks (rarely as dikes in the Sybille pluton). Dikes in the anorthosite are most common within a kilometer or less of the contact with the Sybille pluton. This particular rock forms a tabular body that is continuous for more than a kilometer.

| | | |
|---|---|---|
| | | Continue west on Wyoming 34. |
| 49.3 | 0.4 | Pull off on the right and walk back 100 yards to view outcrops on the north side of the road. |

**Stop 2.4: Porphyrtic Monzonite.** This is a monzonitic rock that contains a fine-grained matrix similar to the rock seen in stop 2.3 with a few percent of isolated alkali feldspar megacrysts. This rock is part of a continuum between the monzodiorite and monzosyenite, which is marked by an increase in the abundance of ternary feldspar megacrysts at the expense of the matrix of plagioclase and ferromagnesian minerals. Associated with the increase in ternary feldspar content is the increase in Fe/(Fe+Mg) content in the ferromagnesian minerals. A reflection of this change is the fact that pigeonite is not present in this rock.

| | | |
|---|---|---|
| | | Return to cars and continue west on Wyoming 34. |
| 51.7 | 2.4 | Pull off on right side of the road and walk back 100 yards to view outcrops on the west side of road. |

**Stop 2.5: Inclusions in olivine-oxide ferrodiorite.** This region exposes a complex series of rocks that we feel represent the roof of the Sybille Monzosyenite. The large hill to the north is a roof pendant of anorthosite that is laced with dikes of olivine-oxide ferrodiorite. The many bulldozer tracks cutting across the face of this hill are prospects that were cut in the Oofdi because the Oofdi appears similar in many ways massive Fe-Ti oxides. However, the Ti content is too low in Oofdi to make them a ore for titanium. The outcrop on the road is hosted in Oofdi and a few nearly fresh examples of this rock can be found if one looks carefully, but most of what one sees are the blocks of anorthosite and high-Al gabbro that are included in the Oofdi.

| | | |
|---|---|---|
| | | Return to cars and continue west on Wyoming 34. |
| 52.5 | 0.8 | As you come to a blind right-hand bend, pull off in wide open are to the left of road (careful of oncoming traffic). Walk across the road to large, fresh road cut. |

**Stop 2.6: Monzosyenite:** This road cut provides a beautiful chance to see the unweathered nature of the monzosyenite that forms the main portion of the Sybill pluton. The rock here consists of megacrysts of K-feldspar, (originally a ternary feldspar), fayalite ($Fa_{98}$), hedenbergite, ilmenite, and quartz (Fuhrman, et al.., 1988). This rock crystallized at very high temperatures (at least 950°C according to Furhman et al, 1988) and at very low

oxygen fugacities (at least 1 log unit below that of the FMQ buffer). Water activity was very low. Fluid inclusions are nearly pure $CO_2$ with densities consistent with entrapment at the conditions of intrusion (3 kb, 950°C). These and the presence of solid inclusions of a Na-KCl solid solution suggest that the Sybille monzosyenite crystallized in the presence of a silicate melt, a salt melt, and a $CO_2$ fluid (Frost and Touret, 1989).

Return to car and continue west on Wyoming 34.

| | | |
|---|---|---|
| 54.0 | 1.5 | Contact between the Sybille and the Archean gneisses. |
| 55.0 | 1.0 | Gate to Exotex ranch (private road). Drive through gate and continue on left branch of ranch road. |
| 55.4 | 0.4 | Stop at meadow. |

**Stop 2.7: Contact aureole at Morton Pass**: This is one of the best-exposed areas of the contact aureole around the Laramie Anorthosite Complex. Temperatures in the aureole ranged from around 700°C at the lower grade portion of the aureole to >900°C near the contact (Russ-Nabelek, 1989; Grant and Frost, 1991; Frost and Frost, 1995).

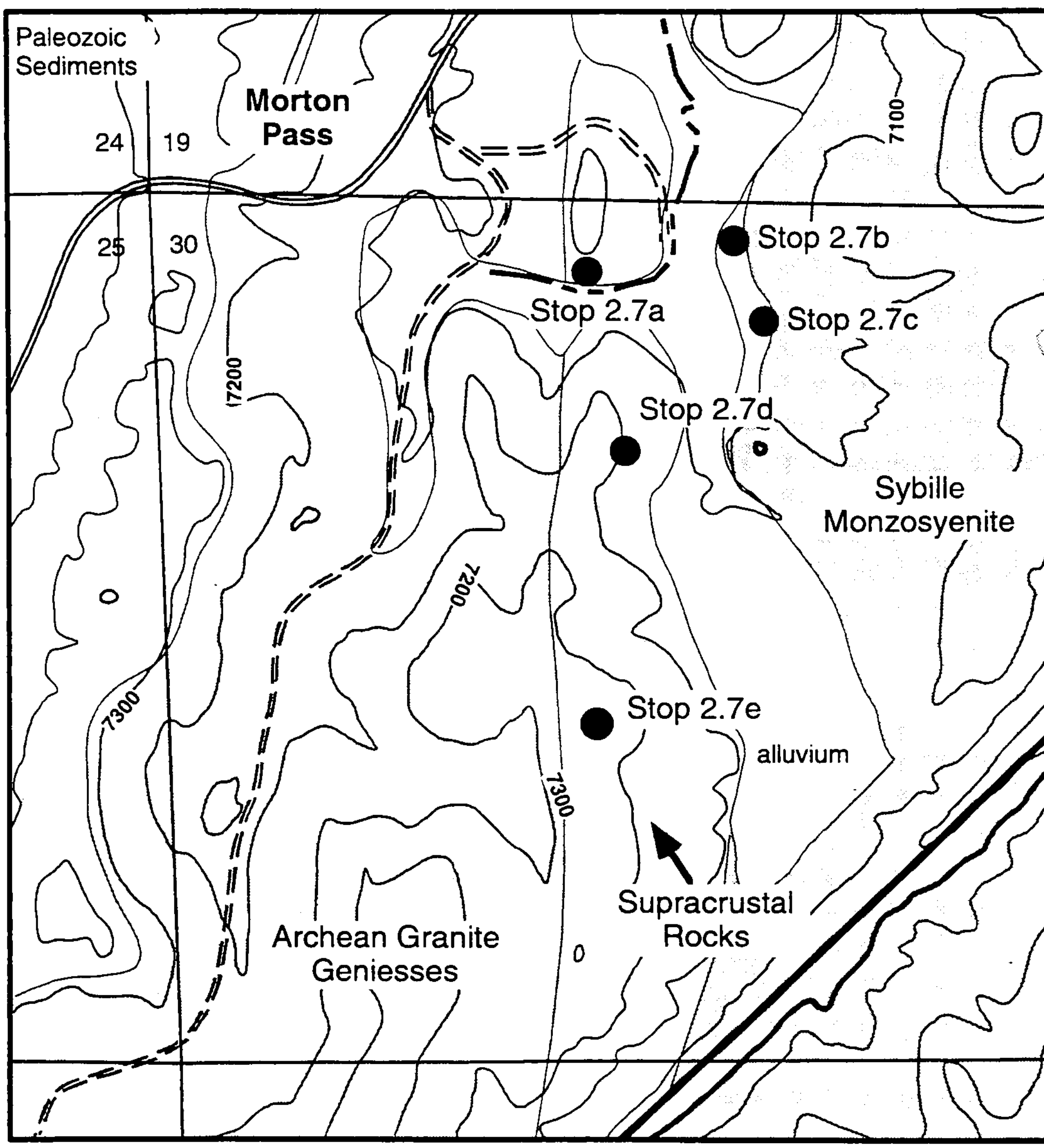


**Figure 17. Geologic sketch map of the Morton Pass areas showing the localities to be visited during the field trip.**

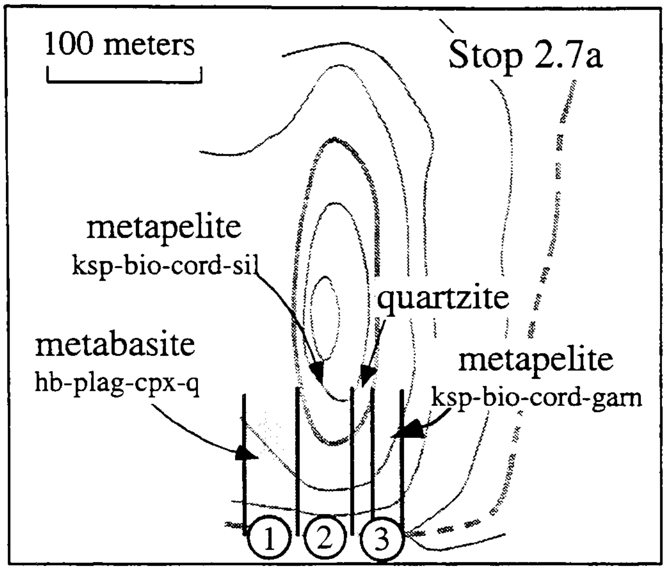


Figure 18. Geologic sketch map of relations at Stop 2.7a.

**Stop 2.7a: "Low-grade" supracrustal rocks.** Walk east to outcrops along the base of a low hill. These outcrops expose a suite of supracrustal rocks that have undergone contact metamorphism by the Laramie Anorthosite Complex. From west to east the rocks are (Figure 18):

**1) Finely banded metabasite.** The most abundant layers are black and hornblende-rich. Interbedded with it are cm-thick or thinner pale green diopside-rich layers, and rare magnetite- and quartz-rich layers are also present. We interpret this as having been derived from an immature sediment of basaltic composition interlayered with carbonate and rare iron-formation. This is the lowest-grade portion of the aureole. The mafic rocks contain the assemblage hornblende-augite-quartz-ilmenite +/- magnetite.

**2) Metapelite.** A few yards further east you come to metapelites that are laced by K-spar rich leucosomes. These rocks have clearly been melted and contain the assemblage Kspar-biotite(Bi)-cordierite(Cor)-plag-quartz. Sillimanite and hercynite may be present in this area, but are rare. The rocks have clearly melted to produce a Kspar-rich melt. Spectacular samples of melt segregating into shear zones have been found as float at this locality.

**3) Metapelite with coexisting cordierite + garnet.** After a thin quartzite layer there are low outcrops of metapelite. This metapelite differs from the first pelitic horizon visited in that granitic melts are less abundant. Furthermore, garnet is present, indicating that we have passed over the reaction:

$$\text{sillimanite} + \text{Bi} = \text{Cor} + \text{garnet} + \text{K-spar (+melt)} \quad (1)$$

Please do not hit the photogenic outcrop with hammers. There is ample collectable material in float.

**Stop 2.7b: High-grade metapelite and the contact with the Sybille pluton.** This knob consists of restitic metapelite from which all melt has been extracted. The mineral assemblage is Kspar-Plag-biotite-opx-cordierite-quartz ± garnet. This assemblage indicates that between here and the last outcrop we have passed over the reaction:

$$\text{quartz} + \text{Bi} + \text{garnet} = \text{Cor} + \text{opx} + \text{Kspar (or melt)} \quad (2)$$

The contact between the metapelites and the Sybille lies along the east side of the hill. Walk along the contact to slabs exposing the Sybille monzosyenite. Even though these slabs are deeply weathered, they show clearly that the Sybille nearer the contact has assimilated quartz and $H_2O$ that has probably been derived from melting generated out of the pelitic rocks.

Walk south from here across a gulch and climb the next hill.

**Stop 2.7c: High-grade metabasite on the contact of the Sybille pluton.** The metabasites that abut the Sybille on this hill are nearly free of hornblende and contain the assemblage opx-cpx-plag-hb. An interesting textural feature in these rocks is the local presence of large hornblendes. We interpret that these hornblendes grew late in the metamorphic history in response to fluids released during the latest crystallization of the Sybille.

Walk west up across meadow and up the hill.

**Stop 2.7d: Metamorphosed supracrustal rocks** As we walk up this hill we will pass over low outcrops and float of metapelite, metabasite, quartzite, and marble. The main assemblage in the metapelite is cordierite-garnet-biotite-Kspar, although, locally quartz-rich horizons are found in which biotite was consumed by reaction (1) and the assemblage is sillimanite-cordierite-garnet. Some beautiful examples of the assemblage hornblende-opx-cpx-plag can be found in the metabasites. The marbles have been strongly retrograded; the most obvious metamorphic mineral is pale yellow serpentine after forsterite. Locally brucite after periclase has been found as well. At the top of the hill we come to the metabasite that we visited initially at Stop 7a. Here the rocks reached a somewhat higher temperature and contain the assemblage hornblende-opx-cpx-ilm ± quartz ± mag.

Continue south along the ridge to the far knob.

**Stop 2.7e: Fluid flushing in metabasite adjacent to marble.** At this locality the metabasite (the same as seen at Stop 7a and 7c) abuts a marble. Adjacent to the marble the metabasite is fine grained and has lost nearly all its hornblende. We interpret that this is due to $CO_2$ moving along a shear zone that was located in the metabasite directly against the marble. The movement of fluids not only induced dehydration of the hornblende, but it also had significant effects on the radiogenic isotope composition of the rocks (Frost and Frost, 1995).

| | | |
|---|---|---|
| | | Return to the vehicles and return to highway. |
| 55.8 | 0.4 | Wyoming 34, turn left, close and lock gate. |
| 56.2 | 0.4 | Morton Pass. |
| 69.1 | 12.9 | Intersection with US 30/287, turn left. |
| 85.8 | 16.7 | Intersection of US30/287 with Curtis Street, Laramie. |

## Day 3: Sherman Batholith

| Total mileage | mileage between points | |
|---|---|---|
| 0.0 | 0.0 | Intersection of US 30 and 30$^{th}$ street. Drive east on US 30. |
| 0.3 | 0.3 | Pass the City Springs on the north side of the road. The springs release water from the Pennsylvanian-Permian Casper Formation, the principal aquifer supplying water for municipal and domestic needs in the Laramie area. The recharge area for the Casper Formation is on the flanks of the Laramie Mountains, seen directly ahead. |
| 0.6 | 0.3 | Wal-Mart building on north side of the road. The building has been built into limestones of the Casper Formation. For the next 0.4 miles US 30 runs parallel to a fault that juxtaposes the Casper Formation on the north, and the Permian Satanka Shale to the south. Stratigraphically above the Satanka shale is the Triassic Chugwater Formation, which forms the dark rusty red outcrops south of the highway opposite Wal-Mart. |
| 1.5 | 0.9 | Pass on to an alluvial fan that is draining west from the Laramie Range. |
| 2.5 | 1.0 | Merge on to I-80 eastbound and shortly after that cross on to the Permian Casper Formation. |
| 4.3 | 1.8 | Enter Telephone Canyon. The Casper Formation consists of buff to reddish well-cemented subarkosic sandstone and interbedded buff limestone. In Telephone Canyon, the Casper sandstone exhibits spectacular large-scale festoon cross-bedding, exposed on both sides of the Interstate for about 2 miles. |
| 8.2 | 3.9 | Happy Jack Exit (Exit #323), turn left at top of ramp and drive over the Interstate. |
| 8.6 | 0.4 | Happy Jack road turns right, continue ahead to Summit Rest Area. |
| 8.9 | 0.3 | Park cars at rest area and walk to building for oversight of the Sherman batholith. Return to cars and drive back to Happy Jack road. |
| 9.5 | 0.3 | Happy Jack road, turn left and follow road across gently dipping surface of the Fountain Formation. |
| 10.4 | 1.2 | Entrance to Tie City Campground. |
| 10.6 | 0.2 | Pass over unconformity between the Paleozoic rocks and the Sherman. |
| 10.9 | 0.3 | Pull over on the right shoulder and walk across to the road cut on north side of the road. |

**Stop 3.1: Typical Medium Grained Sherman Granite.** The Sherman granite is a coarse-grained, subporphyritic granite that is the most common lithology in the batholith. It generally has a reddish-orange color and commonly weathers to a thick grus. The granite is composed of megacrystic potassium feldspar crystals in a matrix of plagioclase, quartz, K-feldspar, hornblende and biotite. Minor phases include sphene, allanite, zircon, and apatite. Trace amounts of fluorite are found locally.

At the north end of the outcrop is a rather poorly exposed granite gneiss. We interpret this as an early, deformed unit of the Sherman batholith, based upon U-Pb zircon ages on similar granite gneisses further east along Sherman Mountain. Bulldozer work during the construction of the road has spread fresh, dynamited samples of this granite gneiss along the base of the entire outcrop.

| | | |
|---|---|---|
| 11.0 | 0.1 | Walk or drive down the road to the next road cut on the north side of the road. |

**Stop 3.2: Texturally Inhomogenous Sherman Granite.** The Sherman granite has an inhomogeneous distribution of mafic minerals, as can be seen at this stop. Although the density of potassium-feldspar megacrysts is relatively constant throughout the outcrop, the matrix ranges from being nearly free of ferromagnesian minerals to being melanocratic. Numerous inclusions of both felsic and mafic rock are present in the outcrop. The mafic enclaves are ferrodioritic in composition, similar to ferrodiorites that are interpreted as residual magmas from the Laramie Anorthosite Complex to the north (Mitchell and others, 1996). We interpret the variation in mineralogy and geochemistry of the Sherman granite to be the result of mixing of a granitic melt with an iron-enriched ferrodiorite component. Further field evidence of magma mixing will be viewed at Stop 5.

| | | |
|---|---|---|
| | | Return to cars and continue east on Happy Jack road. |
| 11.4 | 0.4 | Pull off on right side of highway about 0.1 mile before turn off to Happy Jack recreation area. Cross road to road cut on north side of the road. |

**Stop 3.3: Porphyritic granite** Porphyritic granite is characterized by alkali-feldspar megacrysts in a finer-grained matrix. It occurs throughout the batholith, and is gradational with Sherman granite. The matrix varies from intermediate to felsic. The major phases present in order of decreasing abundance are microcline, plagioclase, quartz, perthite, biotite, and amphibole. The alkali feldspar megacrysts commonly have euhedral cores, with quartz and fluid inclusion filled rims. Mafic enclaves are

common within the porphyritic granite. At this stop some of the mafic enclaves have a gneissic texture. The porphyritic granite is interpreted as a hybrid rock, formed by the interaction of ferrodiorite and felsic melts.

| | | |
|---|---|---|
| | | Return to cars and continue east on Happy Jack Road. |
| 11.5 | 0.1 | Road to Happy Jack recreation area goes off to the right. Turn in here and turn around and head back west on Happy Jack Road. |
| 13.8 | 2.3 | Intersection with road to Summit Rest Area, turn left and continue straight ahead past the access road to the rest area. |
| 14.1 | 0.3 | Pavement ends. The road becomes Headquarters road (Forest Service Road 705), low outcrops on either side are of Fountain Formation. |
| 14.3 | 0.2 | Cross over the Paleozoic unconformity to the Sherman Batholith. |
| 16.0 | 1.7 | Park cars on right side of the road and cross to low outcrops on the north side of road. |

**Stop 3.4: Lincoln Granite.** The Lincoln granite is a medium-grained granite with a low ferromagnesian mineral content. Alkali-feldspar megacrysts are rare to absent. The orange-red granite weathers readily to an orange-brown soil. In most occurrences, the Lincoln granite forms sheets, small plugs, or dikes, and appears to post-date the coarser-grained Sherman and porphyritic granites.

| | | |
|---|---|---|
| | | Return to cars and continue southeast along Headquarters road. |
| 16.9 | 0.9 | Pull out into open area on the right of the road adjacent to a string of beaver ponds. Walk across the road to a series of low outcrops in the sage brush. |

**Stop 3.5: Mingled Melts.** On this hillside there are a series of outcrops displaying varying degrees of interaction between Fe-rich monzodiorite and granite. In most places at this outcrop, the granite is Lincoln granite. Contacts between the Lincoln granite and monzodiorite are lobate and cuspate. The monzodiorites may have rounded, pillow-like forms bounded by Lincoln granite. These types of contacts have been interpreted by other workers as resulting from the commingling of magmas. The sharp contact between the monzodiorite and the Lincoln granite, and the fine grain size of the monzodiorite suggests rapid cooling. In some places the monzodiorites have been brecciated by small veins of Lincoln granite, suggesting that the granites remained above their solidus after the monzodiorites had cooled sufficiently to behave brittlely.

The porphyritic granites are also found in these areas of commingling, and exhibit contacts with the monzodiorite similar to those of the Lincoln granite. In some places elongated spheroids of mafic magma are entrained into the porphyritic granite. Enclaves of Sherman granite are locally found within the porphyritic granite as well. Alkali feldspar mantled with plagioclase, megacryst $^{87}Sr/^{86}Sr$ isotopic compositions that differ from those of the whole rock porphyritic granite values, straight line relationships on Harker variation diagrams, and the field evidence for hybridization all suggest that the process of magma mixing is important in the formation of the porphyritic granite.

| | | |
|---|---|---|
| | | Return to the cars and continue southeast along Headquarters road. |
| 17.7 | 0.9 | Pass Wallis campground on the right. |
| 18.6 | 0.9 | Forest Service Road 707 leads off to the left, stay on 705, which runs straight ahead. |
| 18.9 | 0.3 | Blair picnic ground road runs off to the left. |
| 21.2 | 2.3 | Intersection with old US 30, turn right. |
| 23.7 | 2.5 | Paved road ends, turn left under Interstate 80 and continue around to the right on access road to Vedauwoo. |
| 24.9 | 1.2 | Turn right toward Vedauwoo picnic ground follow road around to the left. |
| 25.9 | 1.0 | End of road in Vedauwoo glen. |

**Stop 2.6: Sherman Granite at Vedauwoo** For our last stop and lunch we are visiting the picnic grounds at Vedauwoo. The rock here is dominated by medium-grained main stage Sherman granite, which contains abundant inclusions of porphyritic granite. A string of inclusions can be seen at the base of the wall on the left side of the road just as the road is entering Vedauwoo glen. Locally isolated inclusions of fine mafic monzonite may also be found.

## REFERENCES


Allmendinger, R.W., Brewer, J.A., Brown, L.D. Kaufman, S., Oliver, J.E. and Houston, R.S. (1982) COCORP profiling across the Rocky Mountain Front in southern Wyoming, Part 2: Precambrian basement structure and its influence on Laramide deformation. Geol. Soc. Amer. Bull., v.93, pp. 1253-1263.

Anderson, I.C. (1995) Petrology and geochemistry of the Red Mountain pluton, Laramie Anorthosite Complex, Wyoming. Ph.D. dissertation, University of Wyoming, Laramie, Wyoming.

Anderson, J.L. (1983) Proterozoic anorogenic granite plutonism of North America, *in* Medaris, L.G. Jr., Byers, C.W., and others, editors, Proterozoic geology: Selected papers from an international Proterozoic symposium. Geol. Soc. Amer. Mem. 161, pp. 131-154.

Bolsover, L.R. (1986) Petrogenesis of the Sybille iron-titanium oxide deposit, Laramie Anorthosite Complex, Laramie mountains, Wyoming. M.S. Thesis, State University of New York, Stony Brook, N.Y.

Darton, N.H., Blackwelder, E., and Siebenthal, C.E. (1910) Laramie-Sherman folio. U.S. G. S. Geologic Atlas of the United States, Folio 173.

Deubendorfer E.M. and Houston, R.S. (1987) Proterozoic accretionary tectonics at the southern margin of the Archean Wyoming Craton. Geol. Soc. Amer. Bull., v. 98, pp. 554-568.

Dymek, R.F., and Gromet, L.P. (1984) Nature and origin of orthopyroxene megacrysts from the St. Urbain anorthosite massif, Quebec. Can. Min., v. 22, pp.297-326.

Eberle, M.M.C. (1983) Genesis of the magnetite-ilmenite deposit at Iron Mountain, Laramie Anorthosite Complex, Wyoming. M.S. thesis, University of Colorado, Boulder Colorado.

Edwards, B.R. (1993) A field, geochemical, and isotopic investigation of the igneous rocks in the Pole Mountain area of the Sherman Batholith, southern Laramie Mountains, Wyoming, U.S.A. M.S. thesis, University of Wyoming, Laramie, Wyoming.

Eggler, D.H. (1968) Virginian Dale Precambrian ring-dike complex, Colorado-Wyoming. Geol. Soc. Amer. Bull., v.79, pp.1545-1564.

Emslie, R.F. (1975) Pyroxene megacrysts from anorthositic rocks: new clues to the sources and evolution of the parent magmas. Can. Min., v. 13, pp. 138-145.

Epler, N.A. (1987) Experimental study of Fe-Ti oxide ores from the Sybille Pit in the Laramie anorthosite, Wyoming. M.S. thesis, State University of New York, Stony Brook, N.Y.

Fountain, J.C., Hodge, D.S., and Hills, F.A. (1981) Geochemistry and petrogenesis of the Laramie anorthosite complex, Wyoming. Lithos, v.14, pp.113-132.

Fram, M.S. and Longhi, J. (1992) Phase equilibria of dikes associated with Proterozoic anorthosite complexes. Amer. Mineral., v. 77, p.605-616.

Frost, B.R., Frost, C.D., Lindsley, D.H., Scoates, J.S., Mitchell, J.N., 1993, The Laramie Anorthosite Complex and the Sherman batholith: geology, evolution, and theories of origin. *in* A.W. Snoke, J.R. Steidtmann, and S. M. Roberts Geology of Wyoming, Geol. Survey of Wyoming Mem. 5, pp.118-161.

_____, Fyfe, W.S., Tazake, K., and Chan, T. (1989) Grain-boundary graphite in rocks and implications for high electrical conductivity in the lower crust. Nature, v.340, pp.134.-136.

_____, and Lindsley, D.H. (1992) Equilibria among Fe-Ti oxides, pyroxenes, olivine, and quartz: Part II. Application. Amer. Mineral., v.77, pp.1004-1020.

_____, Lindsley, D.H., Andersen, D.J., (1988) Fe-Ti oxide - silicate equilibria: Assemblages with fayalitic olivine. Amer. Mineral., v.73, pp.727-740.

_____, and Simons, J.P. (1991) Fe-Ti oxide deposits of the Laramie Anorthosite Complex: Their geology and proposed economic utilization. *in* B.R. Frost, and S. Roberts, Eds. Wyoming Geol. Ass, Forty-Second Field Conference Guidebook, pp. 41-48.

_____, and Touret, J.R.L. (1989) Magmatic CO2 and saline melts from the Sybille monzosyenite, Laramie Anorthosite Complex, Wyoming. Contrib. Mineral. Petrol., v. 103, pp.178-186.

Frost, C.D., Meier, M., and Oberli, F. (1990) Single-crystal U-Pb zircon age determination of the Red Mountain pluton, Laramie Anorthosite Complex, Wyoming. Amer. Mineral., v.75, pp.21-26.

Fuhrman, M.L., Frost, B.R., and Lindsley, D.H. (1988) Crystallization conditions of the Sybille Monzosyenite, Laramie Anorthosite Complex, Wyoming. Jour. Petrol., v. 29, pp. 699-729.

Geist, D. J., Frost, D. C., and Kolker, A. (1990) Sr and Nd isotopic constraints on the origin of the Laramie Anorthosite Complex, Wyoming. Amer. Mineral. v. 75, pp. 13-20.

Grant, J.A., and Frost, B.R. (1990) Contact metamorphism and partial melting of pelitic rocks in the aureole of the Laramie Anorthosite Complex, Morton Pass, Wyoming. Am. Jour. Sci., v. 290, pp. 425-472.

Hild, J.H., 1953, Diamond drilling on the Shanton magnetite-ilmenite deposits,, Albany County, Wyoming. U.S. Bureau of Mines Report of Investigations 5012.

Houston, R.S, Duebendorfer, E.M., Karlstrom, K.E., and Premo, W.R. (1989) A review of the geology and structure of the Cheyenne belt and Proterozoic rocks of southern Wyoming. *in* Grambling, J.A. and Tewksbury, B.J. eds., Proterozoic geology of the southern Rocky Mountains. Geol. Soc. Amer. Special Paper 235, p. 1-12.

Karlstrom, K.E., and Houston, R.S. (1984) The Cheyenne belt: analysis of a Proterozoic suture in southern Wyoming. Precambrian Res., v. 25, pp.415-446.

Kolker, A., Frost, C.D., Hanson, G.N., and Geist, D.J. (1991) Neodymium, strontium, and lead isotopes in the Maloin Ranch Pluton, Wyoming: Implications for the origin of evolved rocks at anorthosite margins. Geochim. Cosmoch. Acta. v. 55, pp.2285-2297,

_____, Lindsley, D. H., and Hanson, G.N. (1990) Geochemical evolution of the Maloin Ranch pluton, Laramie Anorthosite Complex, Wyoming: Trace elements and petrogenetic models. Amer. Mineral., v. 75, pp. 572-588.

_____, and Lindsley, D.H. (1989) Geochemical evolution of the Maloin Ranch pluton, Laramie Anorthosite Complex, Wyoming: Petrology and mixing relations. Amer. Mineral., v. 74, pp. 307-324.

Johnson, R.A., Karlstrom, K.E., Smithson, S.B., and Houston, R.S., (1984) Gravity profiles across the Cheyenne Belt, a Precambrian crustal suture in southeastern Wyoming. Jour. of Geodynamics, v.1, p. 445-472.

Lafrance, B., John, B.E., and Scoates, J.S. (1996) Syn-emplacement recrystallization and deformation microstructures in the Poe Mountain anorthosite, Wyoming. Contrib. Mineral. and Petrol., v. 122, pp. 431-440.

Lindsley, D.H., and Frost, B.R. (1992) Equilibria among Fe-Ti oxides, pyroxenes, olivine, and quartz: Part I. Theory. Amer. Mineral., v.77, pp.987-1003.

Longhi, J., Fram, M.S., Vander Auwera, J., and Montieth, J.N. (1993) Pressure effects, kinetics, and rheology of anorthositic and related magmas. Amer. Mineral., v.78, pp. 1016-1030.

Mitchell, J.N. (1993)Petrology and geochemistry of dioritic and gabbroic rocks in the Laramie Anorthosite Complex, Wyoming: Implications for the evolution of Proterozoic anorthosite. Ph.D. dissertation, University of Wyoming, Laramie, WY.

_____, Scoates, J.S., and Frost, C.D. (1995) High-Al gabbros in the Laramie Anorthosite Complex, Wyoming: implications for the composition of melts parental to Proterozoic anorthosite. Contrib. Mineral. Petrol., v.119, pp.166-180.

_____, Scoates, J.S., Frost, C.D., and Kolker, A. (1996) The geochemical evolution of anorthosite residual magmas in the Laramie Anorthosite Complex, Wyoming. Jour. of Petrol., in press.

Morse, S.A. (1975) Plagioclase lamellae in hypersthene, Tikkoatokhakh Bay, Labrador. Ear. Planet. Sci. Lett., v.26, p. 331-336.

Myers, J.D., Marsh, B.D., and Sinha, A.K. (1985) Strontium isotopic and selected trace element variations between two Aleutian volcanic centers (Adak and Atka): implications for the development of arc volcanic plumbing systems . Contrib. Mineral. Petrol., v. 91, pp. 221-234.

Newhouse, W.H., and Hagner, A.F. (1957) Geologic map of anorthositic areas, southern part of Laramie Range, Wyoming. U.S.G.S. Mineral Investigations Field Studies MF-119.

Premo, W.R. and Van Schmus, W.R. (1989) Zircon geochronology of Precambrian rocks in southeastern Wyoming and northern Colorado. *in* Grambling, J.A. and Tewksbury, B.J. eds., Proterozoic geology of the southern Rocky Mountains. Geol. Soc. Amer. Special Paper 235, pp.13-32.

Raedeke, L.D. and McCallum, I.S. (1980) A comparison of fractionation trends in the lunar crust and the Stillwater Complex. Proceedings of the Conference on Lunar Highlands Crust, pp. 133-153.

Ramarathnam, S. (1962) Geology and petrology of the south portion of the Laramie Anorthosite mass, Albany County, Wyoming. Ph.D. dissertation, Colorado School of Mines, Golden, CO.

Resor, P. G., Chamberlain, K.R., Frost, C.D., Snoke, A.W., Frost, B.R. (1996) Direct dating of deformation: U-Pb age of sphene growth in the Proterozoic Laramie Peak shear zone. Geology, in press.

Scoates, J.S. (1994) Magmatic evolution of anorthositic and monzonitic rocks in the Mid-Proterozoic Laramie Anorthosite Complex, Wyoming, U.S.A. Ph.D Dissertation, University of Wyoming, Laramie, WY.

_____, and Chamberlain, K.R. (1995) U-Pb baddeleyite and zircon ages of anorthositic rocks in the Laramie Anorthosite Complex, Wyoming. Amer. Mineral., v.80, pp.1317-1327.

_____, J.S. and Frost, C.D., 1996, A strontium and neodymium isotopic investigation of the Laramie anorthosites, Wyoming, USA: Implications for magma chamber processes and the evolution of magma conduits in Proterozoic anorthosites. Geochim. Cosmochim. Acta. v. 60, pp. 95-107.

_____, Frost, C.D., Mitchell, J.N., Lindsley, D.H., and Frost, B.R. (1996) A residual melt origin for monzonitic rocks in Proterozoic anorthosite complexes: the Sybille intrusion, Laramie anorthosite complex, Wyoming. Geol. Soc. Amer. Bull., in press.

Spicuzza, M.J. (1990) High grade metamorphism and partial melting in the Bluegrass Creek Suite, Central Laramie Mountains, Wyoming. M.S. Thesis, University of Minnesota, Duluth MN.

Vasek, R.W. (1995) Field, petrographic and geochemical study of magma mixing in the Virginia Dale ring dike, Colorado Front Range. M.S. thesis, University of Nebraska, Lincoln NE.

Verts, L.A., Chamberlain, K.R., Frost, C.D. (1996) U-Pb sphene dating of metamorphism: the importance of sphene growth in the contact aureole of the Red Mountain Pluton, Laramie Mountains, Wyoming. Contrib. Min. Petrol., in press.

TOC